# Variance Gamma process as degradation model for prognosis and imperfect maintenance of centrifugal pumps

Marwa Belhaj Salem, Mitra Fouladirad, Estelle Deloux

# Variance Gamma process as degradation model for prognosis and imperfect maintenance of centrifugal pumps

Marwa Belhaj Salem [b], Mitra Fouladirad [a,b,*], Estelle Deloux [b]

[a] Aix Marseille Université, UMR CNRS 7340, M2P2, Centrale Marseille, France
[b] ICD-M2S, University of Technology of Troyes, France

ARTICLE INFO

*Keywords:*
Variance Gamma
Stochastic Degradation model
Statistical inference
Remaining useful life estimation
Prognostic
Sensitivity analysis
Estimation error propagation
Imperfect maintenance

ABSTRACT

This paper considers the degradation modelling of a non-monotonous health indicator. A Variance Gamma process is proposed for the degradation modelling and its calibration in presence of data is discussed. The remaining useful lifetime estimation based on this model is considered and its sensitivity to parameters estimates is analysed. The model is applied to real data of leakage rate of centrifugal pump. Eventually, an imperfect maintenance policy is proposed and optimized.

## 1. Introduction

Nowadays, highly reliable and safe systems are the key priorities of the advanced industries. The main concern of engineers and researchers is to increase the reliability of systems. A good reliability analysis is essential to predict the failure of the system and to propose an efficient maintenance strategy. The major task of the maintenance strategy is to propose an appropriate model that can replicate the degradation of the system and thereby provide a better system life time prediction [1–7]. Since the stochastic processes are capable to integrate the temporal uncertainty associated to the evolution of degradation, they are widely used in system degradation modelling [8–12]. Gamma and Wiener process are the most used stochastic processes in reliability analyses for modelling the system's degradation.

Gamma process is used when the system degradation shows a monotonic trend and its mathematical computations are relatively tractable [11,13–15]. The inverse Gaussian process is also a good candidate to model a monotonic degradation [12,16]. Even though, the degradation of several industrial systems exhibit a non-monotonic behaviour due their advanced and complicated working conditions, for instance deterioration of asphalt roads presented in [17]. In that aspect, Wiener process is extensively used in modelling the degradation of the system witnessing a non-monotonic behaviour. The fact that the major properties of this process are explored is considered as an advantage [18]. The Wiener process with drift has also been extensively used in degradation modelling. However, there are a lot of non monotonic degradation cases where the Wiener process cannot be fit, for instance a degradation with skewed or large tail increment distribution [19–25]. As a consequence, the requirement of introducing and analysing new sophisticated stochastic processes capable of modelling non-monotonic system's degradation become significant. The Variance Gamma process (VGP) is a good candidate to model a non-monotonic degradation when the Wiener process is not suitable. The increments of a VGP follows a variance gamma distribution also called generalized Laplace distribution or Bessel function distribution. This distribution having four parameters is a normal variance–mean mixture where the mixing density is the gamma distribution. The expression of all the moments is available and Seneta [26] investigated the data fitting problem on VGP by moment method. Fiorani [27] tested the ability of the VGP to model different non-monotonic trend for time series data. Daal and Madan [28] implemented the VGP to determine how much this model can improve the fitting to real data compared to some diffusion and jump–diffusion processes. Seneta [29] presented a review paper on VGP. Yoo [30] proposed the VGP as a robust model for non-monotonic phenomenon with skewed distribution increments. In several studies, the VGP was compared to different models in order to prove its ability to model different data, refer to [31–35].

The main contribution of this paper is as follows.

- The proposition of the Variance Gamma Process (VGP) as degradation model;

* Corresponding author at: Aix Marseille Université, UMR CNRS 7340, M2P2, Centrale Marseille, France.
*E-mail address:* mitra.fouladirad@centrale-marseille.fr (M. Fouladirad).

- Numerical comparison of two likelihood approximation methods for VGP parameter estimation;
- Giving an overview of failure time distribution calculation related to VGP;
- Analyse of the parameters estimates uncertainty on the prognosis results (remaining useful lifetime estimation);
- Calibration and prognosis on leakage rate data of centrifugal pumps;
- Application of an imperfect condition-based policy on centrifugal pumps considering a VGP as degradation model.

First, definition and the properties of the VGP will be presented and a brief literature review will be given in Section 2. Different analysis such as parametric estimation, the failure time distribution and the sensitivity of the VGP paths to its parameters will be introduced. In Section 3, different analysis and the impact of estimation error on failure time distribution are investigated using simulated degradation data. In Section 4, the real data sets retrieved from the centrifugal pump degradation will be presented and analysed. An imperfect maintenance strategy and cost estimation analysis will be proposed in Section 5. Conclusion of the paper will also be presented in Section 6.

## 2. Variance gamma process

In this section, the definition, the properties of the proposed VGP and a brief literature review will be detailed. Different analysis such as parametric estimation, the first hitting time distribution and the sensitivity of the VGP to its parameters will be introduced.

### 2.1. Definition and properties

The VGP is obtained by evaluating Brownian motion (with constant drift and volatility) at a random time change given by a gamma process. VGP was initially introduced as a new stochastic process in finance by Madan and Seneta in 1990 [36]. The process is a pure jump process, having an infinite number of jumps in any interval of time and as a jump Lévy process can be approximated by a compound Poisson process. Unlike Brownian motion, the sum of the absolute variations of VGP is finite which permits it to be written as the difference of two increasing processes. This process increments follow a variance gamma distribution which is skewed and non zero kurtosis which is not the case of the most stochastic processes modelling non-monotonic degradations [37–40]. Since VGP can be acquired by evaluating a brownian motion with drift at a random time given by a gamma process there are four parameters involved in its transition probability. In comparison to a diffusion processes used for non-monotonic degradation modelling, the volatility of the time change process (gamma process) and the drift of the brownian motion are the two additional parameters that permit to control the kurtosis and the skewness [41].

Consider a stochastic process $(W(t))_{t\geq 0}$. If $W(0) = 0$ and the non-overlapping increments are independent and moreover $W(t) - W(s) \sim \mathcal{N}(0, t-s)$, the process $(W(t))_{t\geq 0}$ is a standard brownian motion. Considering the process $(B(t;\theta,\sigma))_{t\geq 0}$ as a brownian motion with drift $\theta \in \mathbb{R}$ and volatility $\sigma > 0$ and $(W(t))_{t\geq 0}$ as a standard brownian motion:

$$B(t;\theta,\sigma) = \theta t + \sigma W(t) \tag{1}$$

Let $(\gamma(t;\mu,\nu))_{t\geq 0}$ be a gamma process with $\frac{\mu^2}{\nu}$ as the shape parameter and $\frac{\mu}{\nu}$ as the scale parameter, where $\mu > 0$ and $\nu > 0$. The VGP at time $t$ can be expressed as:

$$X(t;\sigma,\nu,\theta) = B(\gamma(t;\mu,\nu),\theta,\sigma) \tag{2}$$

As it is mentioned, the VGP is considered as a process of finite variation which can allow it to be presented also as the difference of two gamma processes. This additional presentation is considered as a big advantage of the VGP. The two gamma processes can present two competitive phenomenon where the first presents the increase in the degradation phenomenon and the second presenting the decreases. Such presentation could be so helpful to describe leakage rate evolution in time. According to Madan [36], with this new presentation, the VGP at time $t$ can also be written as follows:

$$X(t;\sigma,\nu,\mu) = \gamma_p(t;\vartheta_p,\nu_p) - \gamma_n(t;\vartheta_n,\nu_n) = \theta\gamma(t;1,\nu) + \sigma b(\gamma(t;1,\nu)) \tag{3}$$

where:

$$\begin{aligned} \vartheta_p &= \frac{1}{2}\sqrt{\theta^2 + \frac{2\sigma^2}{\nu}} + \frac{\theta}{2} \qquad \nu_p = \left(\frac{1}{2}\sqrt{\theta^2 + \frac{2\sigma^2}{\nu}} + \frac{\theta}{2}\right)^2 \nu \\ \vartheta_n &= \frac{1}{2}\sqrt{\theta^2 + \frac{2\sigma^2}{\nu}} - \frac{\theta}{2} \qquad \nu_n = \left(\frac{1}{2}\sqrt{\theta^2 + \frac{2\sigma^2}{\nu}} - \frac{\theta}{2}\right)^2 \nu \end{aligned} \tag{4}$$

Based on the presentation of VGP in (2), the probability density function of $X(t;\sigma,\nu,\mu)$ is given by $f_{X(t;\sigma,\nu,\theta)}$ as follows:

$$f_{X(t;\sigma,\nu,\mu)}(x) = \int_0^\infty \frac{1}{\sigma\sqrt{2\pi g}} \exp\left(-\frac{(x-\theta g)^2}{2\sigma^2 g}\right) \frac{g^{\frac{t}{\nu}-1}\exp(-\frac{g}{\nu})}{\nu^{\frac{t}{\nu}}\Gamma(\frac{t}{\nu})} dg \tag{5}$$

where $\Gamma$ is the Euler Gamma function and by Gradshetyn and Ryzhik [42] this form is integrable.

So far the VGP is mostly used in financial analysis. However, it has possible potentials to be applied in several other applications, especially in the system engineering and maintenance field. The VGP, due to its four parameters, is a flexible stochastic model capable of fitting to different time series with independent increments and non-monotonic paths. VGP can be also expressed under two presentations: the first as a changing time of a brownian motion by a gamma process and the second as a difference of two gamma processes. These characteristics will permit it to model different system's degradation behaviour. The VG simulation is carried out according to three possibilities. In the general case, a gamma process is generated with gamma bridge sampling to give the time set and afterwards a Wiener process for this latter is generated by gaussian increments. In the second method, a Dirichlet bridge sampling is used to generate the difference of two gamma processes. And finally, for the specific cases, two gamma process are generated with gamma bridge sampling and the VGP as their difference is proposed, refer to [40].

### 2.2. Parametric estimation

The estimation of the VGP parameters has not received much attention. Most of the work was based on simulated data [43] and lately few works presented some estimation based on a huge data set. Rathgeber et al. [34] considered a huge daily finance data for 20 years of companies in order to estimate the VGP parameters. Le Courtois and Walter [44] tried to study the estimation of the VGP parameters modelling financial data over the period around 8 years by maximum likelihood method and no computational problems was reported. Cervellera and Tucci [45] attempted to replicate the results of estimation of VGP parameters obtained by Madan et al. [41]. The computational problems, mainly associated with finding the maximum likelihood estimation (MLE) of the parameters of the VGP was investigated. Estimation of the VG parameters is considered as a challenging task because of the complexity of log-likelihood function which contains many local optima and the presence of the modified Bessel function of the third kind. A new expectation–maximization (EM) algorithm was developed by Bee et al. [46] based on expectation-conditional-maximization (ECM) proposed by Nitithumbundit and Chan [47]. The VGP is considered as a good model in fitting data related to a non-monotonic phenomenon and is flexible enough to fit to the skewness and leptokurtosis.

Given a sample of increments $y = (y_1, \ldots, y_n)$, the observed log-likelihood of VGP is given by:

$$L(\mu,\sigma,\theta,\nu;y) = \sum_{k=1}^{n} \log(f(y_k;\mu,\sigma,\theta,\nu)), \tag{6}$$

where $f(y;\mu,\sigma,\theta,\nu)$ is the probability density function given in (3). The log-likelihood function derived [48] is given as follows:

$$L(\mu,\theta,\sigma,\nu;y) = \frac{T}{2}\log\left(\frac{2}{\pi}\right) + \sum_{k=1}^{n}\frac{(y_k-\mu)\theta}{\sigma^2} - \sum_{k=1}^{n}\log(\Gamma(a)\theta) + \sum_{k=1}^{n}\log\left(K_{\nu-0.5}\left(\frac{\sqrt{2\sigma^2+\theta^2}\,|y_k-\mu|}{\sigma^2}\right)\right) + \sum_{k=1}^{n}\left(\mu-\frac{1}{2}\right)\left(log(|y_k-\mu| - \frac{1}{2}log(2\sigma^2+\theta^2)\right) \quad (7)$$

where $K_a$ is the modified Bessel function of the third kind of order $a > 0$. Since one of the parameters to be estimate is inside the modified Bessel function $K_a$, an approximation of this latter is required. The modified Bessel function approximation and therefore the estimation of the parameters in this paper is ensured using two numerical tools. For the first tools, called 'VG' the estimation of the parameters of the VGP can be insured using the 'vgFit' function developed under R [49]. The second tool known as the 'ghyp' uses the 'fit.VGuv' function developed under R [48]. In the VGP, the vgFit function allows the user to employ the Nelder–Mead, the BFGS method (Broyden–Fletcher–Goldfarb–Shanno) or a Newton-type algorithm in estimating the parameters. Since The variance-gamma distributions form a subclass of the generalized hyperbolic distributions, the ghyp method proposes a detailed functionality for working with Generalized Hyperbolic processes such as the VGP. It provides also a fitting method based on the fit.VGuv function that capable to ensure the estimation based only on the Nelder–Mead algorithm. Other approximations are also available for instance on MATLAB.

### 2.3. Failure time distribution

It is of a great interest to assess the evolution of the degradation and to predict the failure to avoid the system failure and an undesirable period of inactivity [1,50]. When the degradation indicator reaches a given threshold known as failure threshold, it means that the system is to much deteriorated and even if it is functioning it cannot fulfil its mission in acceptable manner. The first passage or hitting time of the failure threshold by the degradation path is considered as the failure time. In stochastic process literature the first time a process exceeds a given threshold is known as first hitting time of the process to the threshold.

The failure time associated to the failure threshold $L$ for a VGP $(X(t;\sigma,\nu,\theta))_{t\geq 0}$ is defined as:

$$T = \inf\{t>0, X(t;\sigma,\nu,\theta)\geq L\} \quad (8)$$

In the VGP, the subordinated time is a non continuous path process known as a gamma process which makes the calculation more challenging. Due to the non continuity of paths, the usual first hitting time of a path continuous process such as Wiener process cannot be applied to VGP [51]. Hurd [52] proposed to calculate the first hitting time of the second kind and it is defined as the first time when the process of time change (gamma) is greater than the failure time of the brownian motion. Let us consider $T^*$ to be the first hitting time of the brownian motion from threshold $L$ which is defined as

$$T^* = \inf\{t>0, B(t;\theta,\sigma)\geq L\}.$$

According to Hurd [52], the first passage time of the second kind of $(X(t;\sigma,\nu,\theta))_{t\geq 0} = (B_{\gamma(t;\mu,\nu)})_{t\geq 0}$ is defined as:

$$t_d^* = \inf\left\{t>0, \gamma(t;\mu,\nu)\geq T^*\right\}. \quad (9)$$

This first hitting time of second kind is illustrated in Fig. 1.

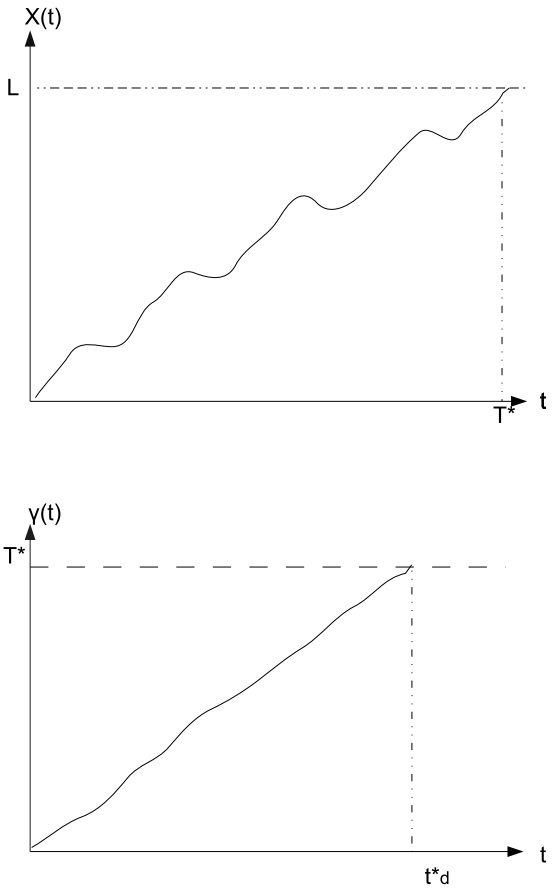


**Fig. 1.** First hitting time of second kind.

The Cumulative distribution function (CDF) of the failure time can also be approximated similarly to the brownian motion first hitting time by another expression as follows :

$$\mathbb{P}(t_d^* < t) \simeq 2\mathbb{P}(X(t;\sigma,\nu,\theta) > L) = 2(1 - F_{X(t;\sigma,\nu,\theta)}(d)) \quad (10)$$

where the $F_{X(t;\sigma,\nu,\theta)}(L) = \int_{-\infty}^{L} f_{X(t)}(x)dx$ and the $f_{X(t)}$ is given by (3).

Li [53] presented another analytical presentation of the first hitting time and $\mathbb{P}(T \leq t)$ can be obtained by calculating the two following equations:

$$\frac{1}{2}\int_0^1\left[1+erf\left(-\frac{\ln(\frac{1}{L})}{\sigma\sqrt{-2\nu\ln(y)}}-\frac{\mu}{\sigma\sqrt{2}}\sqrt{-\nu\ln(y)}\right)\right].\frac{(-\ln y)^{\frac{t}{\nu}-1}}{\Gamma(\frac{t}{\nu})}dy \quad (11)$$

$$\frac{1}{2}\exp\left(\frac{-2\mu\ln(\frac{1}{L})}{\sigma^2}\right)\int_0^1\left[1+erf\left(-\frac{\ln(\frac{1}{L})}{\sigma\sqrt{-2\nu\ln(y)}}+\frac{\mu}{\sigma\sqrt{2}}\sqrt{-\nu\ln(y)}\right)\right] .\frac{(-\ln y)^{\frac{t}{\nu}-1}}{\Gamma(\frac{t}{\nu})}dy \quad (12)$$

According to Li [53], The sum of (11) and (12) provides a new expression of the CDF of first hitting time of the threshold $L$. Once the failure time distribution is obtained a deep study of the model parameters and the impact of the uncertainty related to their estimation on the prognosis.

### 2.4. Remaining useful lifetime distribution

Consider that the system is not failed at time $t$, the remaining time to reach the failure threshold is called remaining useful lifetime at time

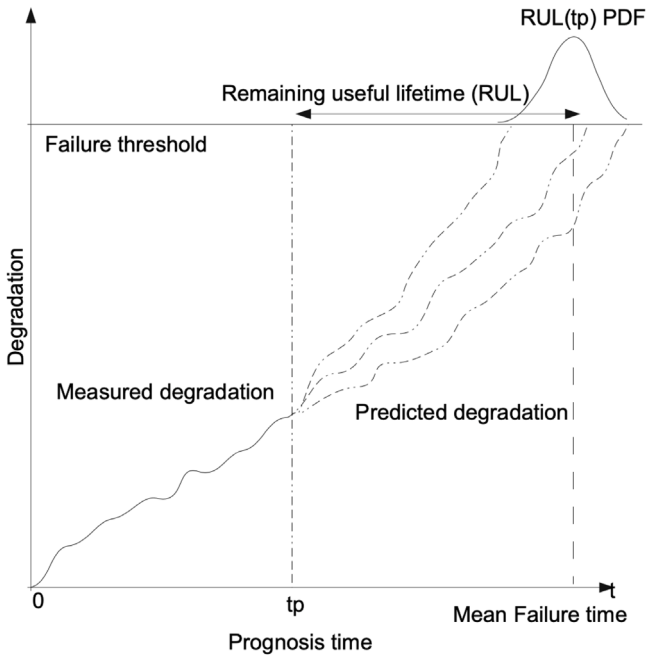


**Fig. 2.** Schematic representation of RUL estimation.

$t$. In other words, the remaining useful lifetime is a random variable indexed by time defined as follows:

$$RUL(t) = \min\{h > 0, X(t+h;\sigma,\nu,\theta) > L | X(t;\sigma,\nu,\theta) < L\}.$$

Therefore,

$$\begin{aligned} F_{RUL(t)}(h) &= \mathbb{P}(RUL(t) \le h) = \mathbb{P}(X(t+h;\sigma,\nu,\theta) > L | X(t;\sigma,\nu,\theta) < L) \\ &= \mathbb{P}(X(t+h;\sigma,\nu,\theta) - X(t;\sigma,\nu,\theta) > L \\ &\quad - x | X(t;\sigma,\nu,\theta) = x < L) \\ &= \int_0^L \mathbb{P}(X(t+h;\sigma,\nu,\theta) - X(t;\sigma,\nu,\theta) > L - x) f_{X(t;\sigma,\nu,\theta)}(x) dx \end{aligned} \tag{13}$$

Fig. 2 explains the first hitting time (FHT) modelling principle. At inspection time $t_{insp}$, the parameters of the past degradation paths are estimated and will be used to calculate the failure time distribution.

In the framework of this paper, the prognosis refers to the RUL distribution estimation at the observation or prognosis time. The main challenge is to define the RUL distribution considering the usage and environmental conditions.

### 2.5. Analysis of the VG parameters on the degradation paths trend

In this section, the impact of the VGP parameters on its paths is analysed. The VGP consist of four parameters, i.e. two extra parameters compared to a brownian motion. The volatility and the drift of the brownian motion are the parameters which control the kurtosis and the skewness of the data. For the increments of the VGP, the mean of is controlled only by the value of the drift ($\theta$), the variance is written as ($\sigma^2 + \nu\theta^2$), the skewness ($\theta\nu(3\sigma^2 + 2\nu\theta^2)/(\sigma^2 + \nu\theta^2)^{3/2}$) and the kurtosis ($3(1 + 2\nu - \mu\sigma^4(\sigma^2))$). From the expression of the mean of VGP, it is obvious that the mean is mainly depending on the drift of the brownian motion $\theta$. It is valuable to study the model's parameters and their impact on the degradation behaviour. A sensitivity analysis was performed by varying the four parameters of the VGP to investigate their influence on the degradation paths (3). For a time horizon $T \in \{600, 10\,000\}$, for each set of parameter, degradation paths are generated. The number of the generated paths can explain the superposition of degradation paths for each set of parameters obtained in (3). The 10 000 trajectories in each figure give an envelop for the process and each trajectory is non-monotonic. It can be noticed that $\theta$ the drift of the brownian motion impacts substantially the degradation path. The volatility parameter of the brownian motion $\sigma$ has not an important impact on the degradation rate. The change of the $\sigma$ value impacts the degradation rate and therefore the failure time. A small value of $\sigma$ implies a slow degradation of the system and delays the time to reach the failure threshold. Similarly, high values of $\sigma$ accelerates the failure threshold reaching.

From 3, one can notice that increasing $\nu$ does not impact the degradation paths. The degradation level for different values of $\nu$ over the period $T = 600$ (hours) reaches the same level of degradation equal to 2000. Same interpretation can be concluded for the parameter $\mu$. For the same time span T = 600 h, the level of the degradation path reach the level 5000 when the values of $\mu$ change. It is confirmed that both $\nu$ and $\mu$ parameters do not have substantial impact on the degradation path trend. As mentioned in Madan [41], when $\theta = 0$ the skewness also will be equal to 0. The expressions of the kurtosis is mainly depending on the parameters $\sigma$, $\mu$ and $\nu$. Since the $\nu$ and $\mu$ parameters have not an important impact on the degradation, the kurtosis can only be presented by $\sigma$.

## 3. Model analysis based on simulated data

In this section, the parametric estimation, first hitting time, prognostics and impact of estimation error of the parameters based on the simulated data were analysed. As explained in the previous section two methods of simulation paths is considered. To generate gamma process with gamma bridge sampling and simulate a Wiener process considering time as the gamma process path. Otherwise two gamma process are generated with gamma bridge sampling or their difference by Dirichlet bridge sampling and the VG as the difference of two gamma processes is derived.

### 3.1. Comparison of maximum likelihood approximation and optimization methods

The parametric estimation of the unknown parameters of the VGP is studied using two approximation of the Bessel function of second kind in software R called VG and ghyp. Different optimization methods are carried out the best results are exposed in this section. The degradation is modelled using the VGP. Different set of parameters are used to generate the degradation paths based on the definition of VGP as an evaluation of the time of the brownian motion with a gamma process. The aim is to define the initial parameters to generate the degradation path and then to estimate these parameters again. The evaluation of the two methods is based on the results of the RMSE (root-mean-square error) calculation for the different number of degradation paths ($N \in \{1000, 10\,000\}$). Each degradation path is generated with a sample length equal to 10 000. The RMSE is obtained by generating the $N$ degradation paths with $n$ points on each path and estimating the four VG parameters. The RMSE of a parameter $\theta$ using the following equation:

$$RMSE = \sqrt{\sum_{i=1}^{N} \frac{(\theta - \hat{\theta}_i)^2}{N}} \tag{14}$$

where $\hat{\theta}_i$ is the estimated parameter from the $i$th trajectory, $N$ is the number of degradation paths and $n$ is the number of data on each trajectory.

The results of the estimation of the two methods for six different VG parameter combinations with $N = 1000$ and $N = 10\,000$ are compared and presented in Tables 1 and 2. Based on the results of the sensitivity of the VGP to its parameters, the six parameters of combinations are chosen to model three types of degradation (slow, average, fast). In this

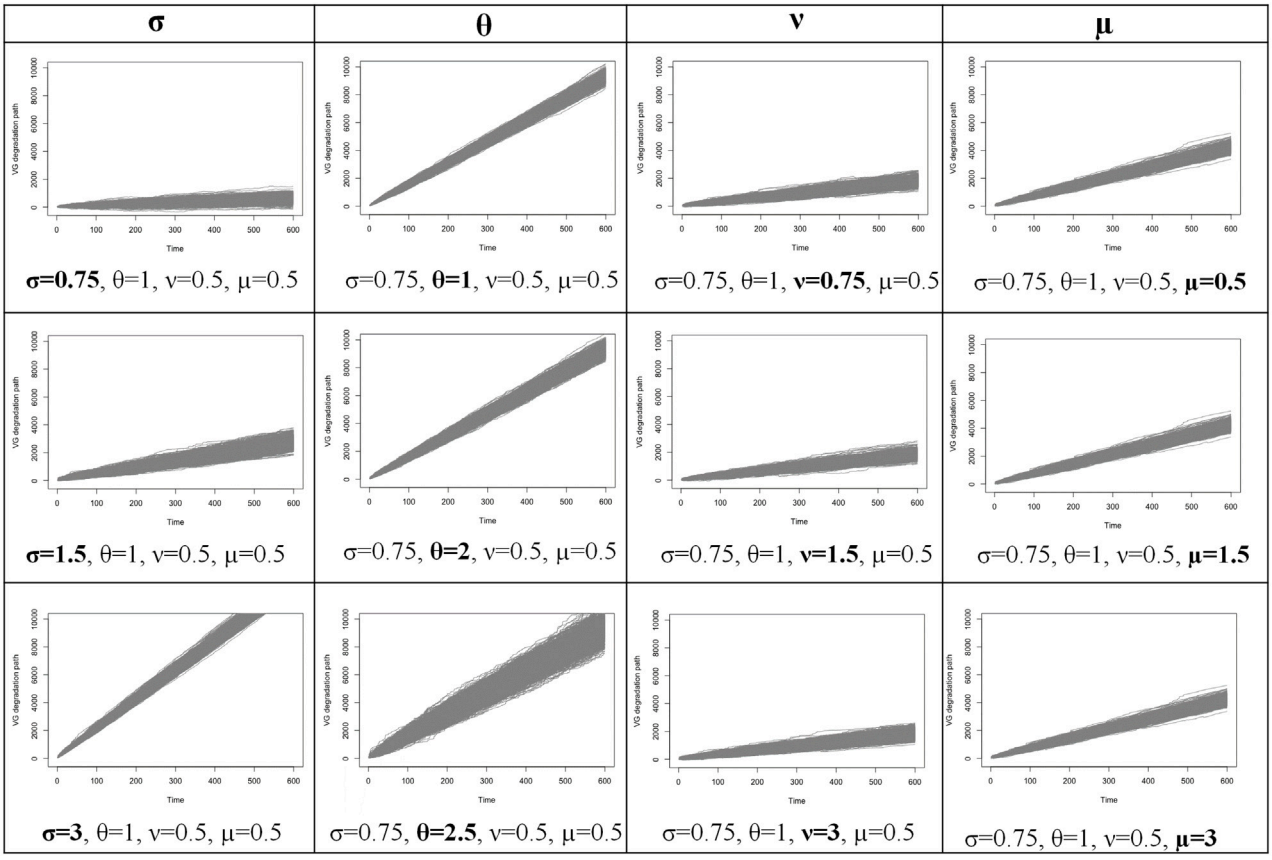


**Fig. 3.** Sensitivity of VG degradation path to each parameter.

**Table 1**
RMSE estimation results ($n = 100$, $N = 1000$).

| | $\mu$ | $\sigma$ | $\theta$ | $\nu$ |
|---|---|---|---|---|
| Real parameters : $\mu = 1$, $\sigma = 2$, $\theta = 2$, $\nu = 1$ | | | | |
| ghyp | 0.0004210789 | 0.00369599 | 0.01053718 | 0.00550920 |
| VGfit | 0.0004551270 | 0.02874830 | 0.03808217 | 0.03849895 |
| Real parameters : $\mu = 1$, $\sigma = 3$, $\theta = 3$, $\nu = 1$ | | | | |
| ghyp | 3.532141e−06 | 0.05741504 | 0.0388627 | 0.2201984 |
| VGfit | 5.612094e−05 | 0.08355467 | 0,0934466 | 0.3364936 |
| Real parameters : $\mu = 1$, $\sigma = 0.75$, $\theta = 0.75$, $\nu = 1$ | | | | |
| ghyp | 0.0004817726 | 0.0004798775 | 0.0008856789 | 0.01186778 |
| VGfit | 0.001164360 | 0.0213160872 | 0.0492638962 | 0.58713126 |
| Real parameters : $\mu = 1$, $\sigma = 1$, $\theta = 1$, $\nu = 1$ | | | | |
| ghyp | 0.001470636 | 0.001535299 | 0.003548021 | 0.006668589 |
| VGfit | 0.003756252 | 0.039027666 | 0.105642000 | 0.135408442 |
| Real parameters : $\mu = 0.5$, $\sigma = 0.25$, $\theta = 0.25$, $\nu = 0.5$ | | | | |
| ghyp | 0.0001100921 | 9.668181e−05 | 0.0002406135 | 0.007128364 |
| VGfit | 0.0051333200 | 1.565608e−03 | 0.0055610143 | 0.063434573 |
| Real parameters : $\mu = 1$, $\sigma = 0.5$, $\theta = 0.5$, $\nu = 1$ | | | | |
| ghyp | 0.0005272317 | 0.0004150291 | 0.001121821 | 0.01069433 |
| VGfit | 0.0021006104 | 0.0147634250 | 0.037662992 | 0.45139110 |

**Table 2**
RMSE estimation results ($n = 100$, $N = 10\,000$).

| | $\mu$ | $\sigma$ | $\theta$ | $\nu$ |
|---|---|---|---|---|
| Real parameters : $\mu = 1$, $\sigma = 2$, $\theta = 2$, $\nu = 2$ | | | | |
| ghyp | 8.295178e−06 | 0.000207052 | 0.009850322 | 3.011430e−04 |
| VGfit | 4.599947e−05 | 0.002201068 | 0.003879024 | 0.007113568 |
| Real parameters : $\mu = 1$, $\sigma = 3$, $\theta = 3$, $\nu = 1$ | | | | |
| ghyp | 1.692809e−07 | 0.0045977 | 0.0082867 | 0.1608650 |
| VGfit | 2.622267e−05 | 0.0640549 | 0.0721939 | 0.2088096 |
| Real parameters : $\mu = 1$, $\sigma = 0.75$, $\theta = 0.75$, $\nu = 1$ | | | | |
| ghyp | 2.316306e−06 | 0.0000379694 | 5.876514e−05 | 0.00076909 |
| VGfit | 6.772278e−05 | 0.0027314184 | 1.310317e−03 | 0.09685972 |
| Real parameters : $\mu = 1$, $\sigma = 1$, $\theta = 1$, $\nu = 1$ | | | | |
| ghyp | 8.500192e−05 | 0.0001453872 | 0.0003301504 | 0.00064286 |
| VGfit | 8.837178e−04 | 0.0032286326 | 0.0006211723 | 0.01124481 |
| Real parameters : $\mu = 0.5$, $\sigma = 0.25$, $\theta = 0.25$, $\nu = 0.5$ | | | | |
| ghyp | 8.644142e−06 | 1.102703e−05 | 2.546313e−05 | 0.0007798861 |
| VGfit | 3.488508e−03 | 3.432321e−04 | 3.460239e−03 | 0.0082440602 |
| Real parameters : $\mu = 1$, $\sigma = 0.5$, $\theta = 0.5$, $\nu = 1$ | | | | |
| ghyp | 2.937456e−05 | 4.663161e−05 | 8.013216e−05 | 0.0007145383 |
| VGfit | 1.624349e−04 | 4.250019e−03 | 2.486369e−02 | 0.1420492314 |

analysis, two Slow, two average and two fast degradations are tested. The two first rows of the Tables 1 and 2 resume the RMSE calculation of a fast degradation parameter. Similarly, the other four rows resumes for average and slow degradation respectively.

For $N = 1000$, the RMSE results obtained by "ghyp" are observed to be smaller compared to the "VG" method and it can be concluded that the method applied in "ghyp" shows better results than the one applied in "VG". Similarly for $N = 1000$, it was noted that the RMSE results for the "ghyp" are smaller as in the case of 1000. The RMSE results using the same data and sample size show that "ghyp" is more efficient in estimation when compared to the "VG" package. However with a fast degradation the two methods efficiency could be similar. It was also perceived that the estimation of the VGP parameters can be affected by the size of used data. In the further analysis, the estimation will be ensured using the "ghyp" R-package and $N = 10\,000$ of degradation paths.

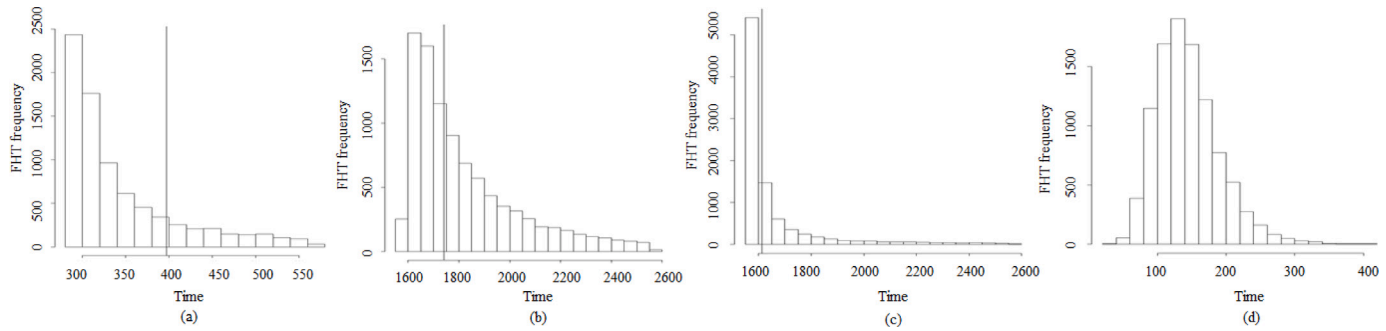


**Fig. 4.** Histogram of the failure time distribution associated to a VGP.

### 3.2. Failure time distribution

In order to carry out a sensitivity analysis, due to burdensome computational time of the closed form approximation methods, Monte Carlo simulation method is used to analyse the failure time distribution. In this aim, our concern is the failure time distribution which is the first hitting time of the failure threshold. For efficiency reasons, different sets of VGP parameters are used to model different types of degradation. The distributions for slow, average and fast degradation rates are studied. Initially, $N = 10\,000$ paths are generated. The paths associated to a fast degradation are generated with the set of parameters VGP($\mu = 1$, $\sigma = 2$, $\theta = 2$, $\nu = 2$). Paths associated to slower degradation are also generated considering VGP($\mu = 0.5$, $\sigma = 0.25$, $\theta = 0.25$, $\nu = 0.5$) and VGP($\mu = 1$, $\sigma = 0.5$, $\theta = 0.5$, $\nu = 1$). The VGP($\mu = 1$, $\sigma = 1$, $\theta = 1$, $\nu = 1$) is introduced to model an average degradation rate. A predefined failure threshold $L$ was defined. The time at which the degradation paths crossing the limit $L$ is captured and used to obtain the histograms of the failure time (4). Fig. 4 presents the obtained failure time histograms for the different degradation paths. The first histogram presents the failure time histogram of an average degradation. The histogram is carried out over a period $T \in [300, 550]$. The failure time of the associated to a fast degradation is obtained over the period $T \in [50, 350]$. For the two slow degradation the histograms of the failure time are obtained on a time span $T \in [1600, 2600]$. The different obtained results show that the histograms of the failure times are unimodal and right skewed. It is essential to study the failure time since it assess the integration of the historical data of the degradation path at the inspection time. The histograms of the failure time provide an idea about the prognostics by locating the real crossing time comparing to the failure time histogram.

It is valuable to evaluate the distribution of the failure time and to investigate its fitting to some famous parametric model. For this fitting, maximum likelihood method is used. Different goodness of fit tests are applied to calibrate the obtained histograms to six parametric models: Weibull, Log-normal, Gamma, Beta, Exponential, Gaussian and Inverse Gaussian models. More precisely, the Kolmogorov–Smirnov, Chi-square, Cramer von Mises and the Anderson–Darling goodness of fit tests are used. Table 3 resumes the results for the different type of degradation (fast, average, slow). All the goodness of fit tests give a very small $p$-value and therefore refused the null hypotheses which means the proposed classical parametric models do not fit the failure time data. The distribution of the failure time provides an idea about the prognostics. The simulation method proposed to obtain the histograms of the failure time is also applied to evaluate the prognostics by considering data from the beginning of the lifecycle until the prognosis time.

**Table 3**
$p$-values of the calibration of the FHT distribution to different laws.

| Law | KS | Chisq | Cramer | AD |
|---|---|---|---|---|
| VG($\mu = 1$, $\sigma = 2$, $\theta = 2$, $\nu = 2$) | | | | |
| Weibull | 0.000415 | 0.026887 | 0.00230 | 0.05051 |
| Log-normal | 0.021345 | 9.281e−04 | 0.006120 | 8.328e−04 |
| Gamma | 2.102e−16 | 0.0001248 | 0.000518 | 1.830e−06 |
| Beta | 7.421e−07 | 0.0006147 | 1.830e−06 | 0.00407 |
| Exponential | 0.00731 | 1.365e−06 | 0.000259 | 0.00873 |
| Gaussian | 8.501e−04 | 3.296e−08 | 9.061e−07 | 0.000749 |
| Inverse Gaussian | 7.304e−06 | 0.000334 | 8.32e−05 | 1.745e−03 |
| VG($\mu = 1$, $\sigma = 1$, $\theta = 1$, $\nu = 1$) | | | | |
| Weibull | 2.752e−12 | 0.000109 | 0.00047 | 6.681e−08 |
| Log-normal | 0.02451 | 0.00934 | 0.00183 | 0.000192 |
| Gamma | 6.851e−05 | 0.00207 | 0.000436 | 3.852e−09 |
| Beta | 2.851e−04 | 1.713e−06 | 9.254e−05 | 6.041e−05 |
| Exponential | 0.00274 | 0.035377 | 0.000219 | 0.000483 |
| Gaussian | 0.02783 | 0.02589 | 4.745e−10 | 9.164e−12 |
| Inverse Gaussian | 0.000164 | 3.841e−07 | 0.002046 | 0.00142 |
| VG($\mu = 1$, $\sigma = 0.5$, $\theta = 0.5$, $\nu = 1$) | | | | |
| Weibull | 0.00409 | 0.014811 | 0.00047 | 0.02783 |
| Log-normal | 2.942e−05 | 9.164e−12 | 0.02589 | 0.000164 |
| Gamma | 0.00029 | 0.00142 | 3.841e−07 | 0.00492 |
| Beta | 0.00081 | 0.045283 | 0.02575 | 0.0002103 |
| Exponential | 0.006317 | 3.076e−09 | 4.185e−08 | 8.43e−07 |
| Gaussian | 0.003051 | 0.01231 | 0.00906 | 0.00035 |
| Inverse Gaussian | 0.00592 | 0.00052 | 3.741e−04 | 0.063845 |
| VG($\mu = 0.5$, $\sigma = 0.25$, $\theta = 0.25$, $\nu = 0.5$) | | | | |
| Weibull | 7.459e−06 | 6.939e−05 | 2.775e−04 | 1.472e−03 |
| Log-normal | 7.053e−08 | 1.472e−03 | 7.053e−08 | 0.00346 |
| Gamma | 0.00346 | 0.000683 | 0.000584 | 2.961e−03 |
| Beta | 0.000735 | 0.00837 | 0.000736 | 0.03515 |
| Exponential | 0.04373 | 1.030e−05 | 0.043042 | 4.863e−08 |
| Gaussian | 0.000653 | 1.965e−05 | 3.965e−04 | 3.745e−06 |
| Inverse Gaussian | 0.002037 | 0.00204 | 0.007031 | 0.00204 |

### 3.3. Prognosis and the impact of parameters estimation error

In this section, the evaluation of the prognosis obtained using the VGP is proposed. Several analyses show that the estimation error in the VG parameters leads sometimes to considerable error in prognosis [54, 55]. In this framework, this section provides a great deal of insight into how estimation errors can impact the performance of the prognosis. Fig. 5 presents the idea of the evaluation of the prognosis by assessing the evolution of the failure time distribution. A degradation path is considered. At the prognosis time, the parameters of the degradation path will be estimated and used to generate a failure time histogram. The idea is to generate a slow degradation path ($D_s$) using the VG($\mu = 0.5$, $\sigma = 0.25$, $\theta = 0.25$, $\nu = 0.5$), mean degradation path ($D_m$) generated with VG($\mu = 1$, $\sigma = 1$, $\theta = 1$, $\nu = 1$) and a fast degradation path ($D_f$) generated using a VG($\mu = 1$, $\sigma = 2$, $\theta = 2$, $\nu = 2$) and to evaluate the prognosis for each degradation path at different inspection times. The first crossing time of the failure threshold for each degradation path is noted as $F_{ct}$ and must be located when the three failure time histograms are obtained. While comparing the position of the $F_{ct}$ with the three failure time histograms obtained respectively at t = $t_{insp1}$, t = $t_{insp2}$ and at $t = t_{insp3}$, the efficiency of the prognosis can be studied. The results obtained at the three prognosis times are presented in 6.

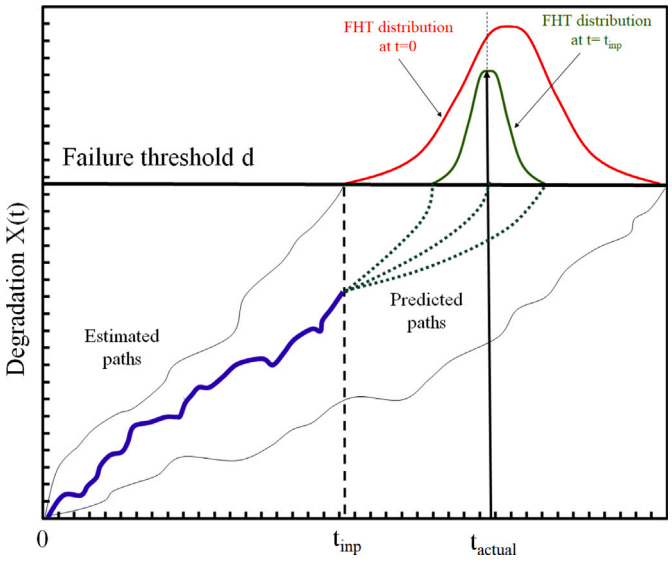


**Fig. 5.** Schematic representation of prognostics based on degradation evolution where FHT represent the failure time.

The first crossing time of the degradation trajectory $F_{ct}$ is presented and compared to the RUL histograms as well as the confidence intervals of 5% and 95% percentiles. Based on the results, one can notice that the $F_{ct}$ of a slow degradation path is well located compared to the failure time histogram and the confidence intervals. Same conclusions can be observed and obtained for the mean and fast degradation paths from the second and third lines of Fig. 6. By evaluating the quality of the RUL estimation, the risk of the failure time estimation after the real failure seems low.

The accuracy of the prognostic is significant for to have a reliable modelling of the system degradation. As a result of this, it is relevant to analyse the impact of estimation error of each VG parameter on prognostics. Moreover, the impact of estimation error can provide a comprehensive sense about the robustness of the estimation algorithms and also to determine the efficiency of the prognostics. Even though it was established that the drift and the volatility parameters are the two parameters which impact the most the degradation of the system, the impact of $\sigma$, $\theta$, $\nu$ and $\mu$ is studied. For one combination of VG parameters, a number $N = 10\,000$ degradation paths are generated in R and the unknown parameters are estimated through maximum likelihood methodm see Table 4). Therefore, for the different four VG parameters, $N$ estimators are calculated their histograms are illustrated in blue in Figs. 7–10.

The objective is to evaluate the distribution of the FHT when the value of the estimator changes. The MLE estimators are asymptotically unbiased and normally distributed. Therefore, the distribution of the estimator can be propagated into the RUL estimation and give the uncertainty at each point of the RUL estimation. The red histograms in 7–10 time to failure histograms for the different quantiles of $\hat{\sigma}$, $\hat{\theta}$, $\hat{\nu}$ and $\hat{\mu}$. More precisely, the $N = 10\,000$ estimated values of $\sigma$ are calculated and the corresponding 10%, 25%, 50%, 75% and 90% quantiles are specified. These quantiles will be used to The evaluation of the impact of estimation uncertainty on the FHT distribution leads to evaluate their impact on prognosis. It can be noticed that considering different quantiles of the parameter estimates does not impact substantially the FHT distribution. Indeed, the estimated variance of parameter estimates are very small he histograms of the FHT did not show remarkable changes when the estimator $\hat{\sigma}$ value which can explain why the estimation error does not impact subsequently the prognosis.

Due to the asymptotic normality of the estimates, delta method leads us to asymptotic normality of the FHT quantiles.

**Table 4**
Summary of parameter estimations ($\sigma = 2$, $\theta = 2$, $\mu = 1$, $\nu = 2$) vector ($N = 10\,000$).

| $\sigma$, $\theta$, $\mu$, $\nu$ | Min | 1st.Qu | Median | Mean | 3rd.Qu | Max | Variance |
|---|---|---|---|---|---|---|---|
| $\sigma$ | 1.905 | 1.928 | 1.980 | 2.015 | 2.074 | 2.112 | 0.0006383893 |
| $\theta$ | 1.8716 | 1.9743 | 1.9989 | 2.0005 | 2.0199 | 2.0536 | 0.0004291118 |
| $\mu$ | 0.9684 | 0.9867 | 0.9340 | 0.9841 | 1.0005 | 1.0012 | 0.0001712903 |
| $\nu$ | 1.9155 | 1.9801 | 1.9947 | 1.9983 | 2.0019 | 2.0035 | 0.0002461708 |

## 4. Application on the real data

Centrifugal pumps are widely used in different small and large industries. The main task of the pump is to transfer fluids from source to destination by providing appropriate pressure (11). The most important parts of the centrifugal pumps are nozzles, shafts, bearings, mechanical seals, impeller, etc.

The mechanical seals are used to provide a leak proof seal between the component parts in centrifugal pumps. Mechanical seals consists of mainly three parts such as o-ring, sealing ring, spring and several sub-parts such as mating rings, flexible diaphragm, retainer, etc. (11). Two degradation factors are identified leading to the failure of seals: delamination of rings and fouling with iron oxide deposit. In order to detect failure the degradation is detected by the monitoring of the leakage rate. A high level of leakage rate will lead to a maintenance action [58]. In this paper, the leakage rate data are retrieved by specific inspections.

The actual retrieved data presenting the health indicator of centrifugal pumps over a specified time period are presented and will be used to confirm the utility of the VGP as a degradation model. The data retrieved presenting the degradation of the centrifugal pump are applied in the calibration of the VGP and to study all its properties. The water leakage rate from the centrifugal pump is considered as the health indicator. The historical degradation data of the centrifugal pump used in this study are retrieved at different periods of the year using different sensors and they present the level of water leakage rate with respect to time, i.e. each 4 h per day. The leakage rate level is considered as a health indicator and a high level of the leakage rate is considered as failure . Four pumps are considered. The retrieved data (leakage rate measurements) are presented gathered in four vectors $V_1$, $V_2$, $V_3$ and $V_4$.

The times series presented by $V_1$, $V_2$, $V_3$ and $V_4$ are considered as degradation paths presented in 12. The monitoring of the degradation is performed over 9 different inspection periods. Let $\left\{ V_{i_j}, i \in \{1, 2, \dots, 9\} \right\}$ be the degradation level of pump $i$ at the $j$th inspection. The centrifugal pump is considered as failed when its leakage rate level is greater than a specific threshold ($d$), The threshold is defined by the experts as a safety level beyond which the system is too damaged to be considered as operational. As soon as the leakage rate of the pump exceeds a failure threshold limit, which is set at around 1400 l/h (litre per hour), the pump is stopped and a corrective maintenance action is performed. Such incident leads to a total shutdown of the operation of the pump, so the engineers proposed to define an alarm threshold in order to propose proactive maintenance decisions. The alarm threshold is set at a level of 1100 l/h. The concept of the alarm threshold is designed to alert the operators to a possible degradation of the pump so it can be maintained early enough before failure. To study the efficiency of the VGP in modelling the non-monotonic degradation behaviour, four goodness of fit tests are applied to the leakage rate dataset. The goodness of fit are applied to give a comparison between the fitting by the VGP and the Wiener process with $p_{value} = 0.05$. The choice of the Wiener process is because it is the most used stochastic processes for modelling non-linear degradation. Since the two processes under consideration are Lévy processes (independent increments) the goodness of fit tests suitable for independent data are applied.

The presented results (5, 6, 7, 8) show that the VGP is more efficient in modelling the centrifugal pump. For the different data set, the

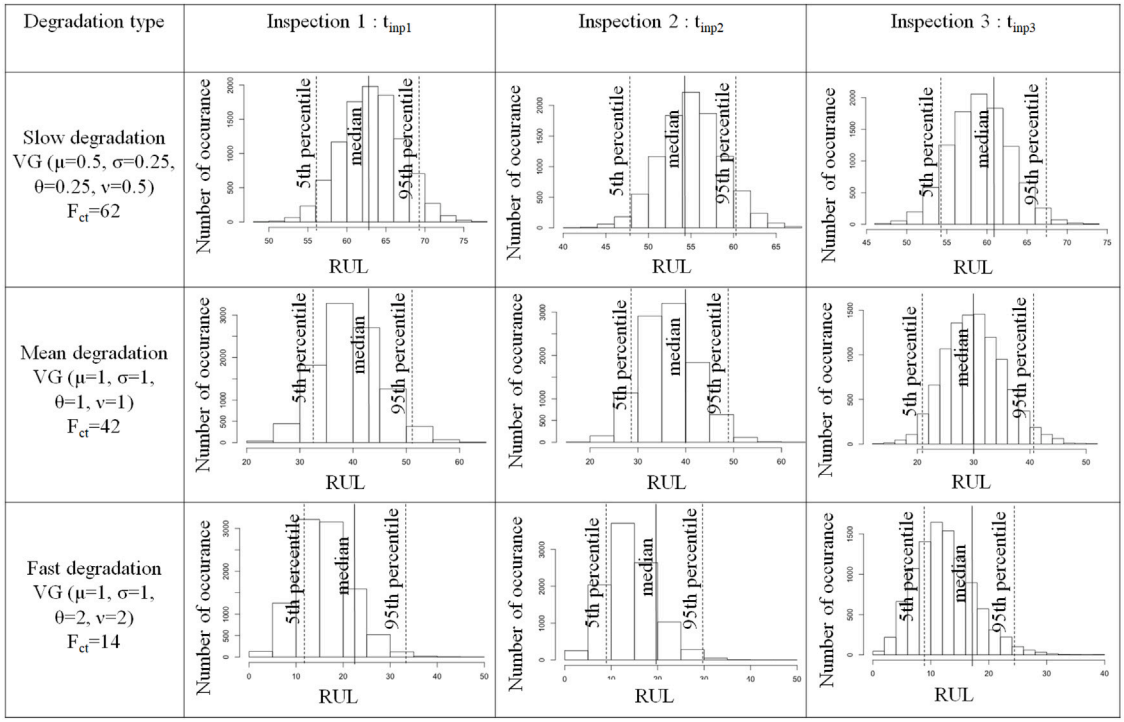


**Fig. 6.** Position of the first crossing time $F_{ci}$ compared to the 5% and 95% percentiles of the failure time histograms obtained at different prognosis times.

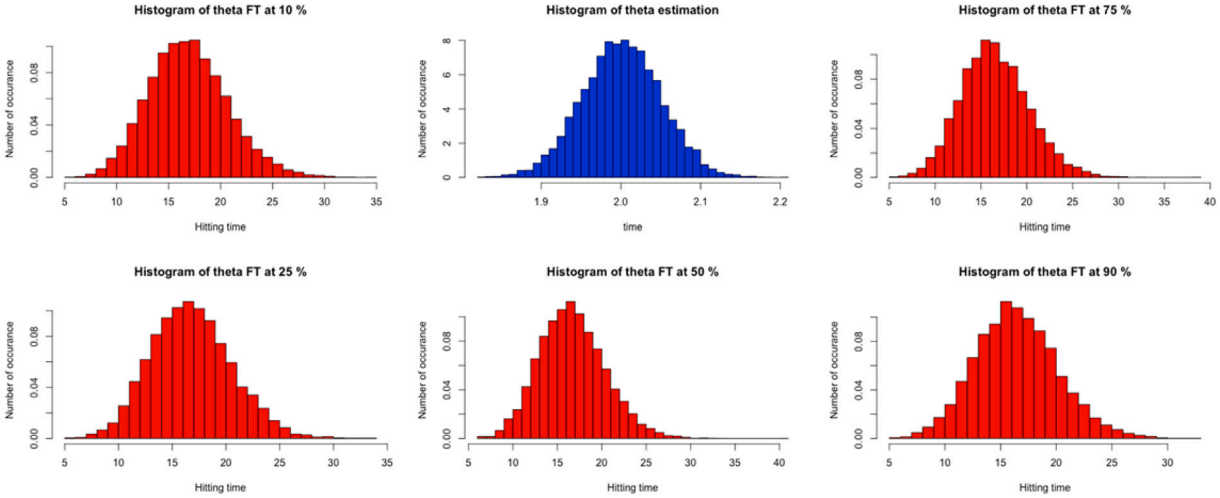


**Fig. 7.** Impact of the uncertainty around the estimator $\hat{\sigma}$ on the failure time distribution, in blue the histogram of $\hat{\sigma}$, in red histograms of failure times for different quantiles of $\hat{\sigma}$.

goodness of fit tests was applied to ensure the calibration of the data to the VG and Wiener process with linear and non linear drift according to the best calibration result. All the goodness of fit tests proved that the VGP is the best process to model such degradation. This can be accepted and explicated by the flexibility of the VGP and its ability to present the small and high jumps on the non-monotonic degradation path. To model the degradation by Wiener process, both the mean and the standard deviation should satisfy some conditions which cannot be accepted or justified for some non-monotonic degradation system [59]. For the sake of confidentiality the parameters of processes are not given.

After ensuring the estimation of the parameters and the calibration of the stochastic model, it is essential to study the FHT distribution and to study the impact of the error of estimations on FHT. These two tasks were performed and the results were combined together and presented Figs. 13, 14, 15. For one specific time span, the four parameters of one real degradation path are estimated. For each VG parameter, due to the asymptotic unbiased and normality of estimates $N$ data are generated but a normal distribution (blue histogram). The values of the estimators will be sorted and then using their values at the different quantiles 10%, 25%, 50%, 75% and 90% a number $N = 10\,000$ of the paths will be generated and the limit threshold is defined. The first hitting time of the limit is captured and used to present the histograms in red. The graphs show that the histogram of the FHT is right skewed and unimodal as in the case of simulated data results. The different graphs are obtained using the same axe scales, for the different parameters the obtained distribution of the FHT occurs in the same time span.

Same work was reproduced with $N = 10\,000$ observations for the other three parameters. As mentioned before, the histograms of the FHT are unimodal and are right skewed. The variance of parameter estimates are very small (less than $2 \times 10^{-4}$) that is why the estimation uncertainty does not influence subsequently the FHT distribution in (9).

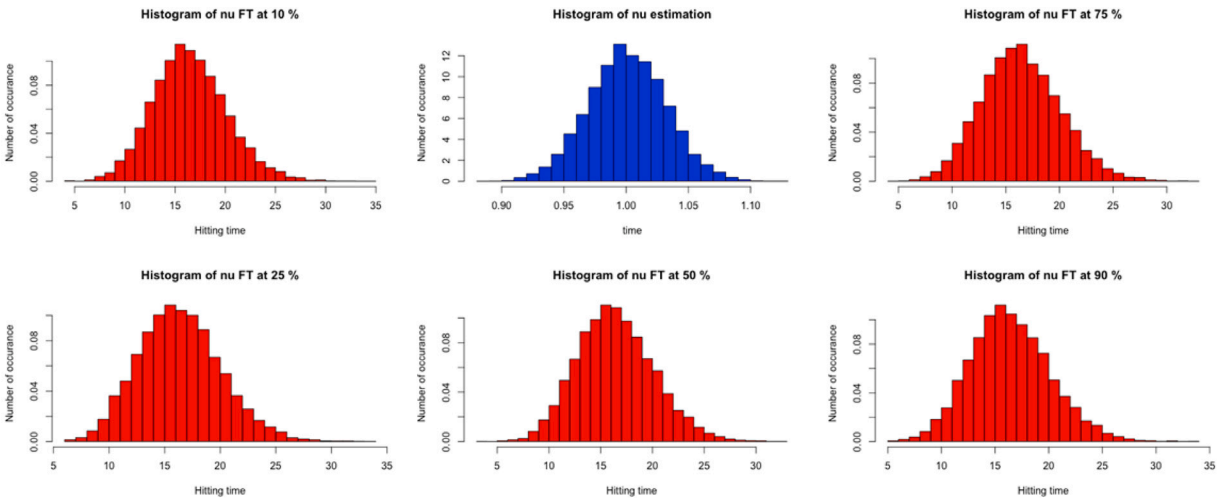


**Fig. 8.** Impact of the uncertainty around the estimator $\hat{\theta}$ on the failure time distribution, in blue the histogram of $\hat{\theta}$, in red histograms of failure times for different quantiles of $\hat{\theta}$.

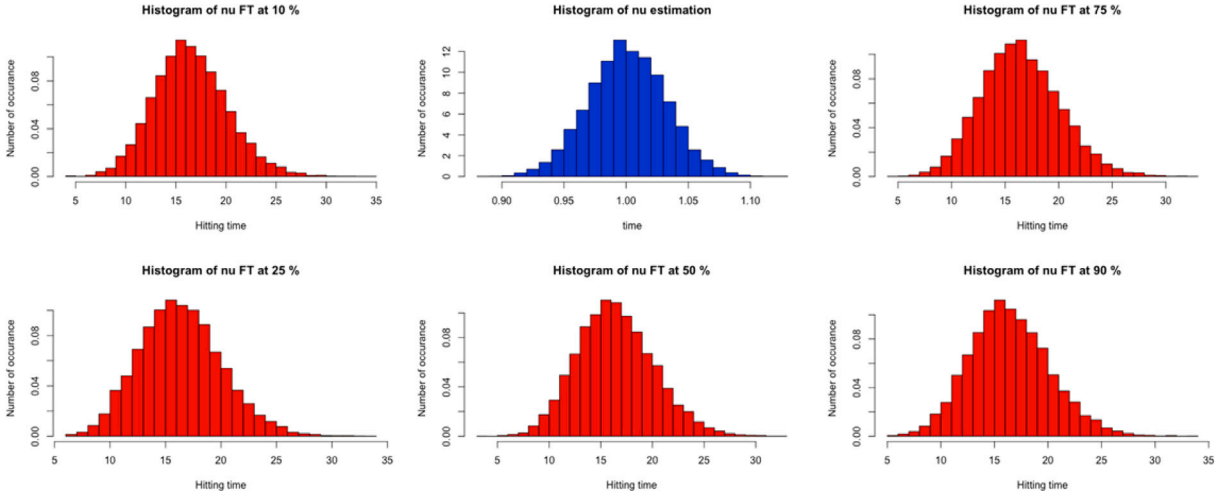


**Fig. 9.** Impact of the uncertainty around the estimator $\hat{\nu}$ on the failure time distribution, in blue the histogram of $\hat{\nu}$, in red histograms of failure times for different quantiles of $\hat{\nu}$.

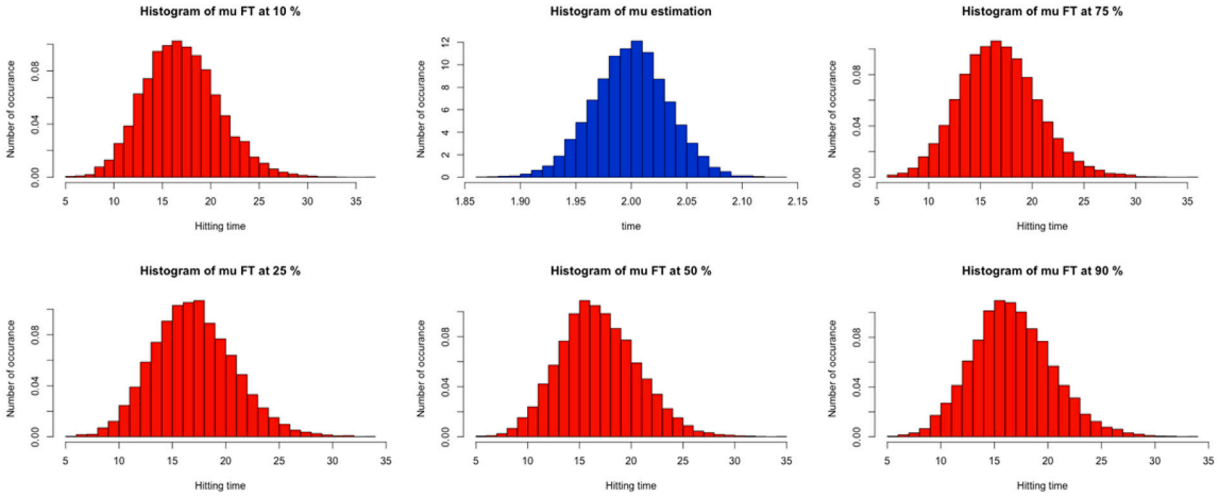


**Fig. 10.** Impact of the uncertainty around the estimator $\hat{\mu}$ on the failure time distribution, in blue the histogram of $\hat{\mu}$, in red histograms of failure times for different quantiles of $\hat{\mu}$.

The next step will be fitting the distribution of the FHT to a parametric model. Four goodness of fit tests are used to approve the fitting with a $p_{value} = 0.05$ : Kolmogorov-test (KS), Chis-square test (chisq), Anderson-test (AD), Cramer-test (Cramer). For each degradation path

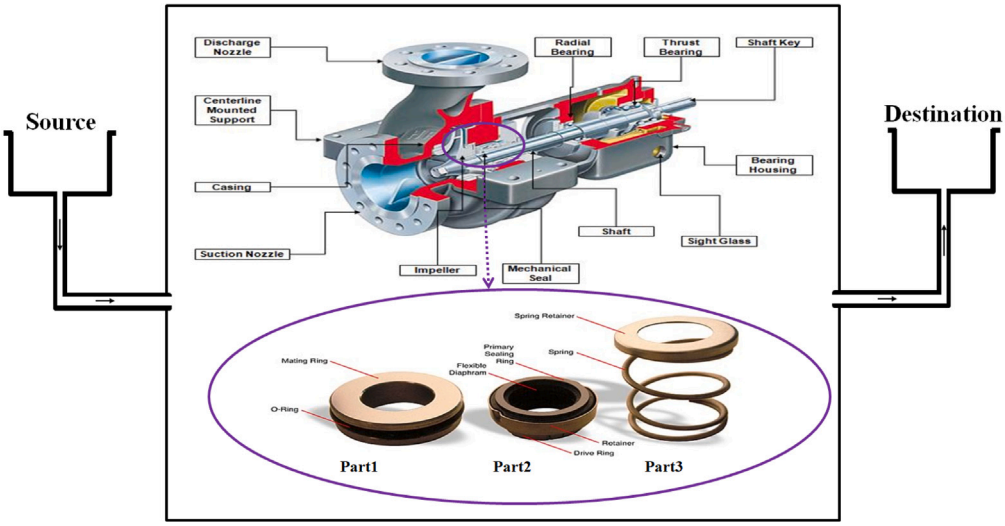


**Fig. 11.** Working principle of centrifugal pump and the detailed presentation of its mechanical seal [56,57].

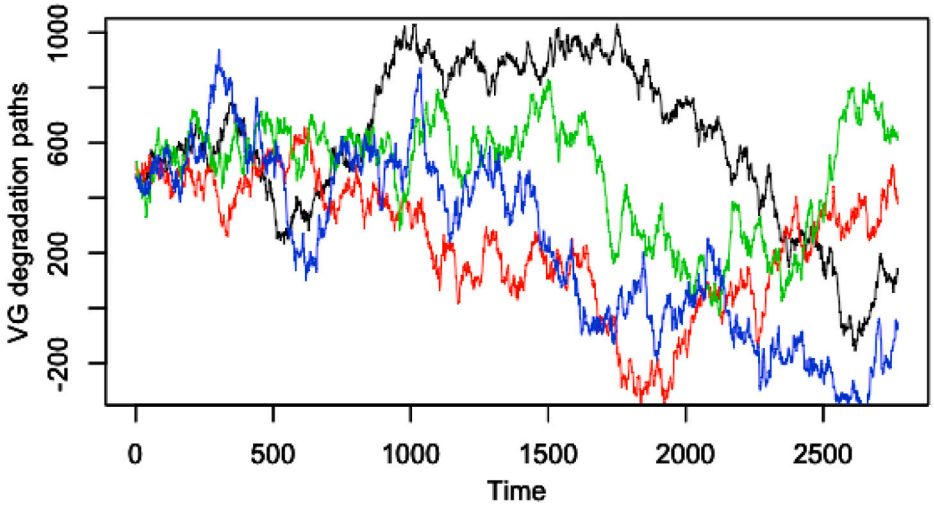


**Fig. 12.** Leakage rate (l/h) of the four systems over a time (h): $V_1$, $V_2$, $V_3$ and $V_4$.

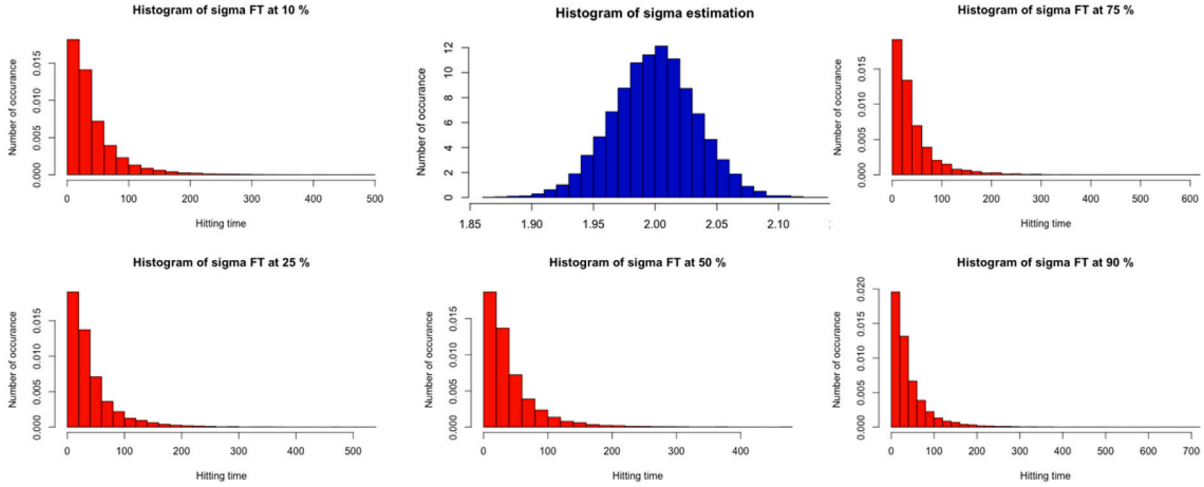


**Fig. 13.** In blue the histogram of $\hat{\sigma}$, in red histograms of failure times for different quantiles of $\hat{\sigma}$.

of ($V_1$, $V_2$, $V_3$ and $V_4$), the process parameters are estimated and then used to generate $N = 10\,000$ paths. When the 10 000 paths of each degradation paths exceeds the failure threshold, the first hitting time is captured and then used to define the distribution of the FHT. The

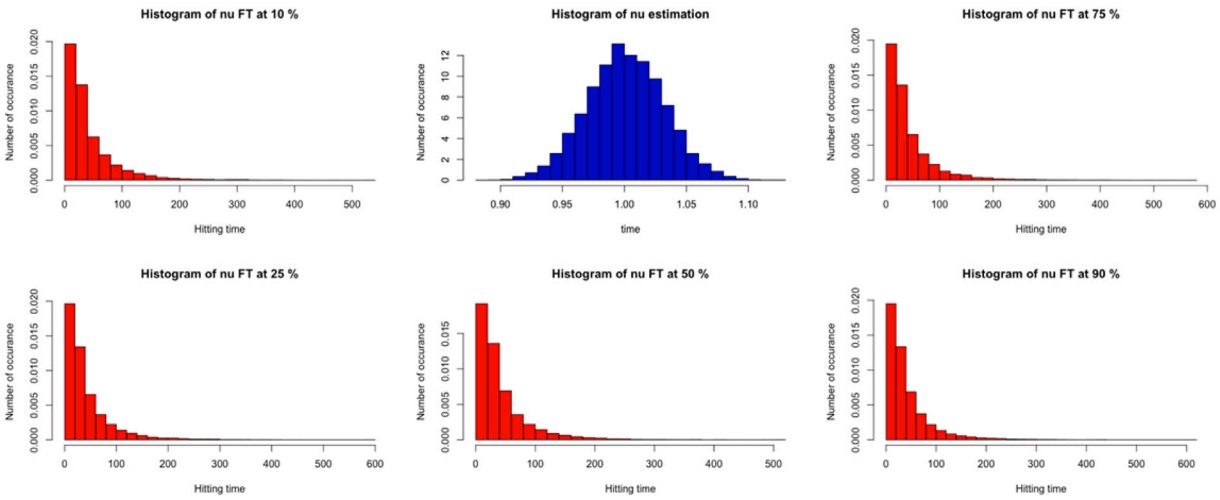


**Fig. 14.** In blue the histogram of $\hat{\nu}$, in red histograms of failure times for different quantiles of $\hat{\nu}$.

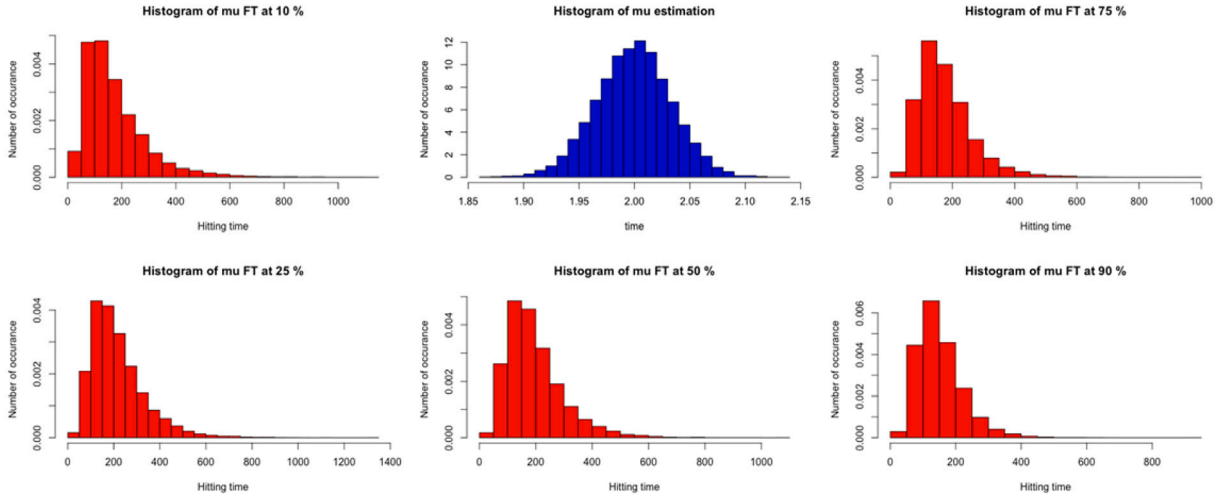


**Fig. 15.** In blue the histogram of $\hat{\mu}$, in red histograms of failure times for different quantiles of $\hat{\mu}$.

**Table 5**
*p*-values for calibration of first vector of real data (V1).

| Pump valve 1 | Process | KS.test | Chisq.test | AD.test | Cramer test |
|---|---|---|---|---|---|
| $V_{1_1}$ | VG | 0.2439 | 0.3876 | 0.3165 | 0.7532 |
| | Wiener | 0.0001854 | 0.026457 | 0.001045 | 8.054e−03 |
| $V_{1_2}$ | VG | 0.2472 | 0.2207 | 0.1847 | 0.3286 |
| | Wiener | 0.00769 | 0.001063 | 0.00907 | 3.938e−04 |
| $V_{1_3}$ | VG | 0.2452 | 0.4309 | 0.7362 | 0.2170 |
| | Wiener | 8.375e−04 | 1.282e−10 | 0.001058 | 3.967e−10 |
| $V_{1_4}$ | VG | 0.6041 | 0.3827 | 0.837 | 0.294 |
| | Wiener | 4.387e−04 | 8.361e−08 | 4.703e−10 | 1.750e−07 |
| $V_{1_5}$ | VG | 0.3097 | 0.5139 | 0.2106 | 0.4739 |
| | Wiener | 0.00902 | 0.001753 | 0.00854 | 0.004015 |
| $V_{1_6}$ | VG | 0.2551 | 0.7014 | 0.8104 | 0.6074 |
| | Wiener | 0.04768 | 0.041981 | 1.047e−06 | 0.032075 |
| $V_{1_7}$ | VG | 0.2408 | 0.063717 | 0.8105 | 0.2601 |
| | Wiener | 0.046628 | 0.039015 | 0.028319 | 0.038938 |
| $V_{1_8}$ | VG | 0.2255 | 0.2419 | 0.2412 | 0.2438 |
| | Wiener | 0.033491 | 0.16179 | 0.00975 | 0.01059 |
| $V_{1_9}$ | VG | 0.2575 | 0.12123 | 0.09654 | 0.2672 |
| | Wiener | 3.438e−05 | 0.010651 | 0.0085832 | 6.455e−05 |

**Table 6**
*p*-values for calibration of second vector of real data (V2).

| Pump valve 2 | Process | KS.test | Chisq.test | AD.test | Cramer test |
|---|---|---|---|---|---|
| $V_{2_1}$ | VG | 0.2408 | 0.2419 | 0.2466 | 0.1619 |
| | Wiener | 0.041981 | 0.04768 | 0.032075 | 0.034434 |
| $V_{2_2}$ | VG | 0.2412 | 0.17594 | 0.3763 | 0.443 |
| | Wiener | 0.00724 | 0.00204 | 0.00937 | 0.01064 |
| $V_{2_3}$ | VG | 0.5216 | 0.803 | 0.2 | 0.07281 |
| | Wiener | 0.7086 | 0.0418 | 6.947e−04 | 0.000381 |
| $V_{2_4}$ | VG | 0.1614 | 0.089 | 0.3785 | 0.3008 |
| | Wiener | 0.02451 | 0.00934 | 0.00183 | 0.000192 |
| $V_{2_5}$ | VG | 0.6229 | 0.4081 | 0.5183 | 0.2419 |
| | Wiener | 0.035377 | 0.044811 | 0.02783 | 0.02589 |
| $V_{2_6}$ | VG | 0.1408 | 0.3844 | 0.17075 | 0.16462 |
| | Wiener | 0.045283 | 0.02575 | 0.0002103 | 0.0006317 |
| $V_{2_7}$ | VG | 0.11263 | 0.088953 | 0.05165 | 0.063845 |
| | Wiener | 0.04853 | 0.006812 | 0.0004647 | 0.034433 |
| $V_{2_8}$ | VG | 0.7225 | 0.52733 | 0.3803 | 0.3553 |
| | Wiener | 0.03515 | 0.04373 | 0.043042 | 0.1511 |
| $V_{2_9}$ | VG | 0.62367 | 0.3313 | 0.7604 | 0.3974 |
| | Wiener | 0.002037 | 0.007031 | 0.028149 | 0.04798 |

**Table 7**
*p*-values for calibration of third vector of real data (V3).

| Pump valve 3 | Process | KS.test | Chisq.test | AD.test | Cramer test |
|---|---|---|---|---|---|
| $V_{3_1}$ | VG | 0.3427 | 0.06231 | 0.7758 | 0.47297 |
| | Wiener | 0.00439 | 0.00091 | 0.00271 | 0.0684 |
| $V_{3_2}$ | VG | 0.9425 | 0.8174 | 0.6703 | 0.10973 |
| | Wiener | 0.00218 | 0.0194 | 0.0405 | 0.00039 |
| $V_{3_3}$ | VG | 0.83 | 0.2408 | 0.2396 | 0.1221 |
| | Wiener | 0.037168 | 0.03008 | 0.000438 | 8.164e−04 |
| $V_{3_4}$ | VG | 0.7031 | 0.5884 | 0.8453 | 0.071355 |
| | Wiener | 0.032058 | 0.03516 | 0.00792 | 0.045502 |
| $V_{3_5}$ | VG | 0.2427 | 0.2694 | 0.2419 | 0.092037 |
| | Wiener | 0.00382 | 0.00184 | 0.0213 | 0.025993 |
| $V_{3_6}$ | VG | 0.10651 | 0.10445 | 0.5561 | 0.3067 |
| | Wiener | 0.027798 | 0.035379 | 0.00903 | 0.00439 |
| $V_{3_7}$ | VG | 0.2405 | 0.2348 | 0.2416 | 0.1312 |
| | Wiener | 0.029135 | 0.01734 | 0.047932 | 0.2519 |
| $V_{3_8}$ | VG | 0.2487 | 0.7572 | 0.1734 | 0.07589 |
| | Wiener | 0.03702 | 0.009534 | 0.004841 | 0.003742 |
| $V_{3_9}$ | VG | 0.3228 | 0.2519 | 0.6342 | 0.4246 |
| | Wiener | 0.04716 | 0.0502 | 0.00735 | 0.000643 |

**Table 8**
*p*-values for calibration of fourth vector of real data (V4).

| Pump valve 4 | Process | KS.test | Chisq.test | AD.test | Cramer test |
|---|---|---|---|---|---|
| $V_{4_1}$ | VG | 0.3419 | 0.13426 | 0.11343 | 0.14236 |
| | Wiener | 0.001854 | 0.01005 | 0.00937 | 0.01002 |
| $V_{4_2}$ | VG | 0.3032 | 0.12037 | 0.10651 | 0.4246 |
| | Wiener | 0.047932 | 1.868e−04 | 0.027798 | 0.000643 |
| $V_{4_3}$ | VG | 0.81062 | 0.00539 | 0.2694 | 0.11582 |
| | Wiener | 0.003086 | 0.06241 | 0.00184 | 0.042599 |
| $V_{4_4}$ | VG | 0. 6354 | 0.000634 | 0.2453 | 0.2207 |
| | Wiener | 0.00762 | 0.047932 | 0.027921 | 0.001063 |
| $V_{4_5}$ | VG | 0.5216 | 0.3876 | 0.2 | 0.4309 |
| | Wiener | 0.7086 | 0.026457 | 6.947e−04 | 1.282e−10 |
| $V_{4_6}$ | VG | 0.1614 | 0.2396 | 0.3785 | 0.7225 |
| | Wiener | 0.02451 | 0.000438 | 0.00183 | 0.03515 |
| $V_{4_7}$ | VG | 0.2405 | 0.089 | 0.3750 | 0.5139 |
| | Wiener | 0.029135 | 0.00934 | 8.705e−04 | 0.001753 |
| $V_{4_8}$ | VG | 0.3313 | 0.2170 | 0.1094 | 0.7014 |
| | Wiener | 0.007031 | 3.967e−10 | 0.004109 | 0.041981 |
| $V_{4_9}$ | VG | 0.2551 | 0.294 | 0.063717 | 0.2207 |
| | Wiener | 0.04768 | 1.750e−07 | 0.039015 | 0.001063 |

**Table 9**
Summary of parameter estimation for real data ($N = 10\,000$).

| Parameter | Min | 1st.Qu | Median | Mean | 3rd.Qu | Max | Variance |
|---|---|---|---|---|---|---|---|
| $\sigma$ | 1.420 | 1.487 | 1.500 | 1.500 | 1.514 | 1.572 | 0.0004599811 |
| $\theta$ | 0.9346 | 0.9841 | 0.9997 | 1.0007 | 1.0164 | 1.0726 | 0.0005493316 |
| $\mu$ | 0.4885 | 0.5261 | 0.5340 | 0.5341 | 0.5425 | 0.5862 | 0.0001570702 |
| $\nu$ | 0.9544 | 0.9900 | 1.0001 | 1.0003 | 1.0115 | 1.0435 | 0.0002350807 |

obtained FHT distribution will be fitted using the four goodness of fit tests to the different parametric models such as Exponential, lognormal, Weibull, Gamma, Beta and the Inverse Gaussian models with $p_{value} = 0.05$. The four FHT distribution fits were performed and the results were presented (10, 11, 12, 13). The FHT distribution did not fit to any of the proposed parametric models. The Gamma, Weibull, exponential, lognormal, beta and inverse Gaussian distributions cannot present a distribution that can model the FHT distribution of a VGP. The FHT density of the VGP has a specific distribution that cannot be modelled using such candidates. This will lead us to the need of using simulation in the rest of the work such as proposing prognostic.

The new advanced systems are operating in a stressed and dynamic environment which will impact the working conditions of the system

**Table 10**
*p*-values for goodness of fit test for FHT data derived on vector ($V_1$).

| Law | KS.test | AD.test | Chisq.test | Cramer test |
|---|---|---|---|---|
| Exponential | 0.04207 | 0.0158 | 0.00571 | 0.02607 |
| Lognormal | 0.005867 | 0.003628 | 0.000491 | 0.006827 |
| Weibull | 0.033617 | 0.002151 | 0.00382 | 0.00184 |
| Gamma | 0.00396 | 0.00902 | 0.001753 | 0.005395 |
| Beta | 4.382e−04 | 0.00047 | 0.00343 | 0.01037 |
| Inverse Gaussian | 0.00115 | 0.03835 | 0.00207 | 0.000751 |

**Table 11**
*p*-values for goodness of fit test for FHT data derived on vector ($V_2$).

| Law | KS.test | AD.test | Chisq.test | Cramer test |
|---|---|---|---|---|
| Exponential | 0.007031 | 0.004109 | 0.041981 | 0.001790 |
| Lognormal | 0.01087 | 0.03668 | 0.00854 | 0.000429 |
| Weibull | 0.002851 | 0.001438 | 0.01095 | 0.00173 |
| Gamma | 0.004762 | 4.072e−04 | 0.04259 | 0.01058 |
| Beta | 0.00745 | 1.055e−07 | 0.00503 | 8.32e−05 |
| Inverse Gaussian | 0.00694 | 0.00493 | 0.02087 | 0.00047 |

**Table 12**
*p*-values for goodness of fit test for FHT data derived on vector ($V_3$).

| Law | KS.test | AD.test | Chisq.test | Cramer test |
|---|---|---|---|---|
| Exponential | 0.1094 | 0.035009 | 0.04219 | 0.00247 |
| Lognormal | 0.002601 | 0.00531 | 0.000806 | 0.01553 |
| Weibull | 0.00759 | 0.00458 | 0.00215 | 0.000672 |
| Gamma | 0.02563 | 0.00581 | 2.12e−06 | 0.001408 |
| Beta | 0.01907 | 2.157e−08 | 0.001048 | 0.005024 |
| Inverse Gaussian | 0.009262 | 0.00164 | 0.071518 | 2.738e−04 |

**Table 13**
*p*-values for goodness of fit test for FHT data derived on vector ($V_4$).

| Law | KS.test | AD.test | Chisq.test | Cramer test |
|---|---|---|---|---|
| Exponential | 0.00507 | 0.001628 | 0.00754 | 0.02593 |
| Lognormal | 0.02402 | 0.01513 | 0.01307 | 0.000681 |
| Weibull | 0.00287 | 0.00521 | 0.00384 | 0.00156 |
| Gamma | 0.00591 | 0.04529 | 0.00103 | 0.0218 |
| Beta | 5.013e−05 | 0.000184 | 0.00751 | 1.250e−07 |
| Inverse Gaussian | 1.128e−08 | 0.00162 | 4.649e−06 | 0.00372 |

that can affect or accelerate its degradation. The usefulness of the VGP in degradation modelling is explored. Both simulated and real data are considered to analyse the VGP statistical properties. As it is one of the first papers proposing the application of the VGP in modelling the system degradation, the possibilities of implementing the VGP in the system maintenance field are opened. Similar works may be recreated in the prediction of degradation of gas pipeline valves, chemical containers, etc.

## 5. Imperfect maintenance strategy and cost estimation analysis

In this section, imperfect maintenance strategy and cost estimation analysis of a system subject to failure will be detailed. An optimization of this strategy will be proposed in order to avoid catastrophic disaster of systems and thereby reduce the maintenance cost for the industries. In this study, two different policies are proposed and the optimal maintenance parameters are obtained to minimize the long-run average maintenance cost. The structure of the maintenance policy is presented to define the proper time of implementing either inspection or replacement activities. Also, the expression of the log-run maintenance cost is developed to propose an optimized maintenance decision. The two proposed maintenance will be applied to the degradation data of the centrifugal pump. As mentioned before, the centrifugal pump system is witnessing a non-monotonic degradation and it is modelled using VGP.

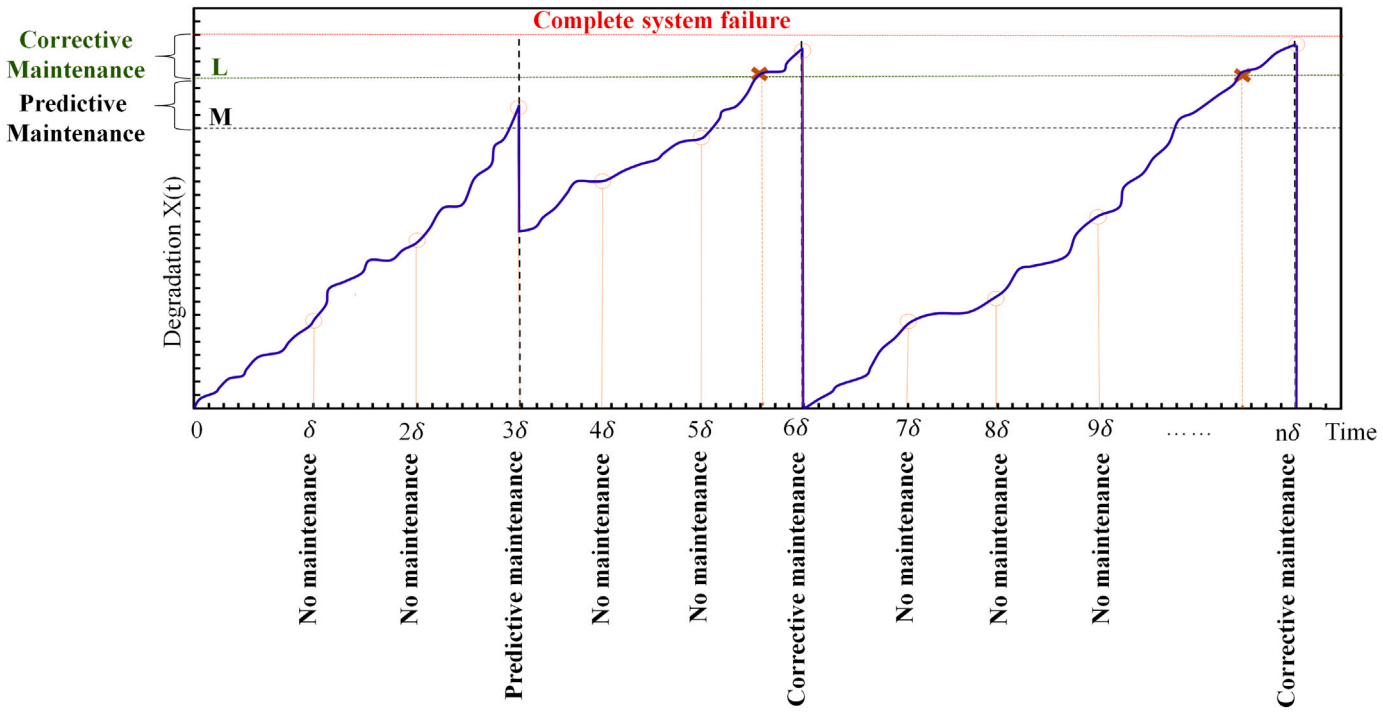


**Fig. 16.** Illustration of the degradation evolution and the imperfect maintenance strategy.

### 5.1. Periodic inspections

The cumulative degradation level of the system $X_t$ cannot be observed and can only be measured by inspections. In this study a periodic maintenance strategy is proposed. It is known that a non-periodic inspections offers optimal results. The system is inspected every $\delta$ and after the replacement of the failed system, it will be inspected at regular time intervals ($\delta$, $2\delta$, …, $n\delta$) until the next replacement.

16 illustrates the degradation evolution and the maintenance strategy. The degradation as a function of time is plotted and the different maintenance actions are presented. Considering the initial case, the degradation level was verified at $\delta$, $2\delta$ and $3\delta$. During the first 2 inspections, the degradation level did not attain the threshold and further inspections were approved. At the third inspection, it was observed that the degradation level crossed the threshold and the level of the degradation is estimated in order to perform the appropriate maintenance action. The level of the system degradation is considered as the health indicator that based on it the maintenance policy will be scheduled. Based on the inherent of the system given by the manufacturers two thresholds were proposed: the first threshold (M) is used as an alarm threshold and the second threshold (L) indicates the total failure of the system. When the level of degradation exceeds the threshold $M$, a preventive maintenance action will be applied. These preventive actions will improve the state of the system and decrease its degradation and leading to an imperfect maintenance. These maintenance actions will lead to an improvement of the system's behaviour with different percentage $P\%$. When the degradation level exceeds the second threshold $L$ a corrective maintenance actions are required. In such cases, it is mandatory to stop the system for corrective maintenance actions. The researchers and the reliability engineers are often keen to optimize this maintenance strategy for a better management of the systems.

### 5.2. Replacements

The corrective replacement which takes place to renew the system after failure or the preventive replacement used to improve the system and avoid the failure presents the two types of replacement that are mainly used. A corrective replacement is required if the system is observed in the failure state during the inspection time. The total cost of the maintenance mainly consists of the cost unit of the corrective replacement $C_c$, the cost unit of the unavailability per unit of time $C_u$, the inspection cost $C_i$ and the cost unit of the preventive replacement $C_p$. The preventive replacement is recommended when the degradation level at the inspection time $X_k$ is between the alarm and the failure thresholds. It is essential to mention that the cost unit of the preventive replacement $C_p$ must be smaller than the corrective replacement cost unit $C_c$. In this study, the parameters of the maintenance decision that should be optimized in order to obtain a minimized long-run maintenance cost are:

- The alarm threshold $M$ leading to avoid the failure.
- The inspection period $\delta$, allowing the optimization of the maintenance cost by evaluating the cumulative inspection cost, the prevention of a failure and the earlier detection.
- The rate of the preventive maintenance $P\%$ leading to an upgrade of the system degradation behaviour.

The study consists of inspecting the system every $\delta$ and at each inspection time. The leakage rate is considered as the degradation level. The leakage rate level will be compared to the two predefined thresholds. For the cases when the leakage rate did not exceed the alarm threshold, only inspection costs will be considered and the system will be working. When the leakage rate reaches the level between the $M$-threshold and the $L$-threshold, a preventive maintenance actions are proposed and the system behaviour will be corrected with a correction percentage given by $P\%$. The cost of the maintenance will be obtained by integrating all the previous inspection costs and the preventive maintenance costs. When the leakage rate exceeds the level $L$, a corrective maintenance actions are needed and the whole system will be replaced. The replaced system will start operating as a new system and the maintenance cost unit will be calculated based on the previous inspection cost unit, the preventive cost unit, the correction cost unit and the unavailability cost unit. The three decision variables are important which implies a better evaluation of their impact on the maintenance cost. The idea is to find a suitable maintenance policy

**Table 14**
Part/Task, price and Mean time to repair (MTTR).

| Part/Task | Price | MTTR |
|---|---|---|
| O-ring | 20 | 20 min |
| Mating ring | 50 | 25 min |
| Flexible diaphragm | 35 | 25 min |
| Primary sealing ring | 55 | 30 min |
| Drive ring | 40 | 30 min |
| Retainer | 70 | 45 min |
| Spring | 60 | 35 min |
| Spring retainer | 30 | 1 h |
| Work force (wf) | 20 | per h |
| Delivery charge (dc) | 5 | per item |
| Production cost loss (plc) | 200 | per h |
| Inspection cost (ic) | 5 | per h |

that offers the best maintenance cost but also is easy to implement. The three parameter estimation has lot of local minima that is why to two parameters optimization is considered. For that two maintenance policies are proposed in order to evaluate the impact of varying the $(M, \delta)$ values comparing to varying the $(M, P\%)$ values. The aim is to find the optimum values of the three decision criteria which lead to an optimum value of the maintenance cost. The first policy $(M, \delta)$ and the policy $(M, P\%)$ are also proposed and evaluated with different values of $(M, \delta)$ and $(M, P\%)$.

### 5.3. Cost-based criterion for maintenance performance evaluation

The mathematical framework for assessing the evaluation of the performance of the proposed maintenance policy with respect to the long-run maintenance cost per unit of time is presented. Let be $C(t)$ the total maintenance cost until time $t$ The total expected maintenance cost acquired by integrating the successive actions operated on the system is given using the following equation:

$$C_{\infty} = \lim_{t \to \infty} \frac{C(t)}{t} = \frac{E(C(T))}{E(T)} \tag{15}$$

where, $T$: a replacement period: between the beginning of the system lifetime cycle and the corrective maintenance.

$E(T)$: the average of the renewal cycle known as:

$$E(T) = \int_0^{\infty} R(t)dt \tag{16}$$

and R(t) is the reliability of the system $R(t) = \mathbb{P}(X_t < L)$. The Cost expectation is derived as follows:

$$E(C(t)) = \sum_{i=0}^{[t/\delta]} C_c \mathbb{P}(X_{\delta i} > L) + C_p \mathbb{P}(M \leq X_{\delta i} \leq L) + C_i + C_u \int_{\delta(i-1)}^{\delta i} f(u)du \tag{17}$$

with $f$ design the probability of failure.

The numerical implementation leading to obtain the optimal values of the decision parameters will be presented. For the better illustration of the strategies, the approximated cost of the each part of the centrifugal pump seal that cause the leakage rate and the cost of different tasks were considered 14. For the same system, the maintenance costs are considered respectively $c_i = 20$, $c_p$ =20, $c_c$ =100 and $c_u$ =30.

The 17 presents the results of the calculation of the maintenance cost. The first graph (a) present the results of the optimization of the maintenance cost unit with respect to the imperfect maintenance actions $P\%$. The optimum value of $P\%$ of 8.3 provided the optimum maintenance cost. Similarly, the second graph (b) presents an evaluation of the maintenance cost to the different values of $\delta$. The optimum cost was obtained for $\delta$ = 4.95. The graph (c) indicates that for $M$ =890, the optimal cost value was obtained. From the numerical results, it can be concluded that the optimum results of the maintenance cost were noticed for $M$ = 890, $P\%$ = 8.3 and $\delta$ = 4.95. If the alarm threshold was settled late after $M$ =880, the maintenance actions will be costly because of the late detection of the failure, which will cause an important period of unavailability and an increase in the maintenance cost.

The two proposed maintenance policies $(M, \delta)$ and $(M, P\%)$ were also evaluated. 18 resume the obtained results of the two policies. The first graph (a) shows that the optimal cost is given with $C_{\infty}(M_{opt} = 1093, P\%_{opt} = 5.3) = 318.45$. The second graph (b) presents also the optimal cost given by $C_{\infty}(M_{opt} = 1075, \delta_t = 4.7) = 310.50$. The two maintenance policies were compared and it is noted that the second policy offered a better optimized cost of maintenance.

## 6. Conclusion

In this study, the VGP is proposed to model the system degradation. Initially, a brief literature review about the evolution of VGP, definition and the properties are presented. The estimation of the unknown parameters of the degradation model is obtained using the two methods: 'VG' and the 'ghyp'. The obtained results of the estimation show that the 'ghyp' method gives the best results. A study of the distribution of Failure Time (FHT) was also performed. The analytical study of the FHT was complicated and due to that the simulation method was proposed as an alternative. The usefulness of the proposed VG model and the importance of integrating a non-linear behaviour into the degradation model was demonstrated. The VGP proved its ability to model a non-linear degradation and as any degradation model, it is important to qualify the nature of prognostic. VG prognostic is studied and the obtained prognostic is evaluated. Moreover, the impact of estimation error on prognostics was also presented. Based on the sensitivity study of the FHT to the error of estimation, one can presume that the VG is proposing an efficient prognostic. The real data sets retrieved from the centrifugal pump degradation were presented as a real study case of the VG modelling. All the works introduced and presented with simulated data were applied on the real data. Two maintenance policies were proposed to optimize the expected total maintenance cost and to evaluate the efficiency of the VGP. Numerical examples show that the performance of the two proposed policies is very promising. In the future, it is important to study the proposed mathematical model in the presence of covariates. It can be relevant to evaluate also the performance of the maintenance policy $(M_{opt}, P\%_{opt}, \delta_t)$.

## CRediT authorship contribution statement

**Marwa Belhaj Salem:** Conceptualization, Methodology, Software, Writing – original draft. **Mitra Fouladirad:** Conceptualization, Methodology, Writing – review & editing. **Estelle Deloux:** Writing – review & editing.

## Declaration of competing interest

The authors declare that they have no known competing financial interests or personal relationships that could have appeared to influence the work reported in this paper.


## Acknowledgement

The authors would like to acknowledge the valuable financial support of the European Regional Development Fund (FEDER) and the Departmental Council of Aube, France during this research.

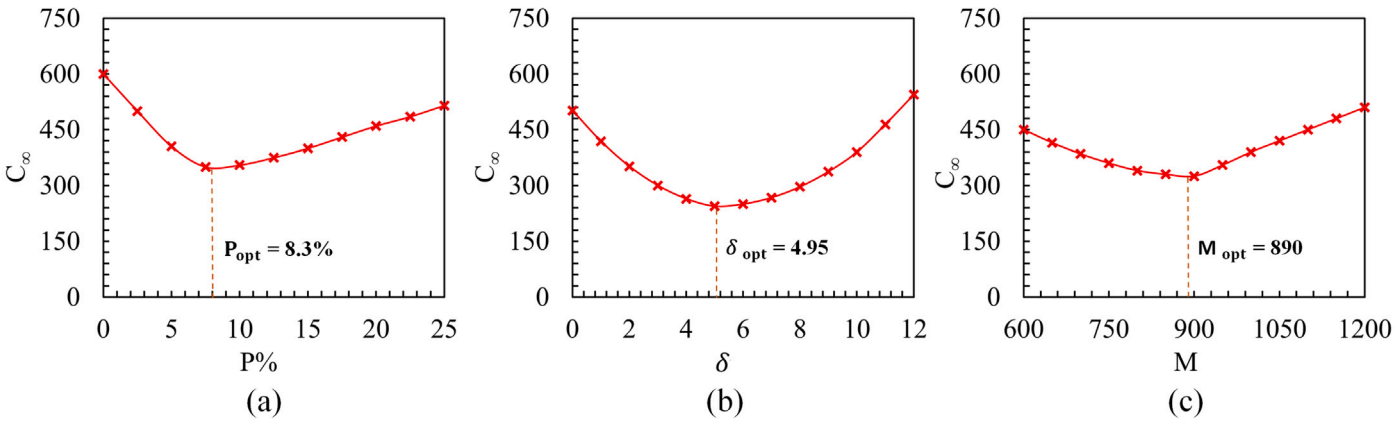


**Fig. 17.** Optimum cost estimation with respect to : (a) $P\%$, (b) $\delta$, (c) $M$.

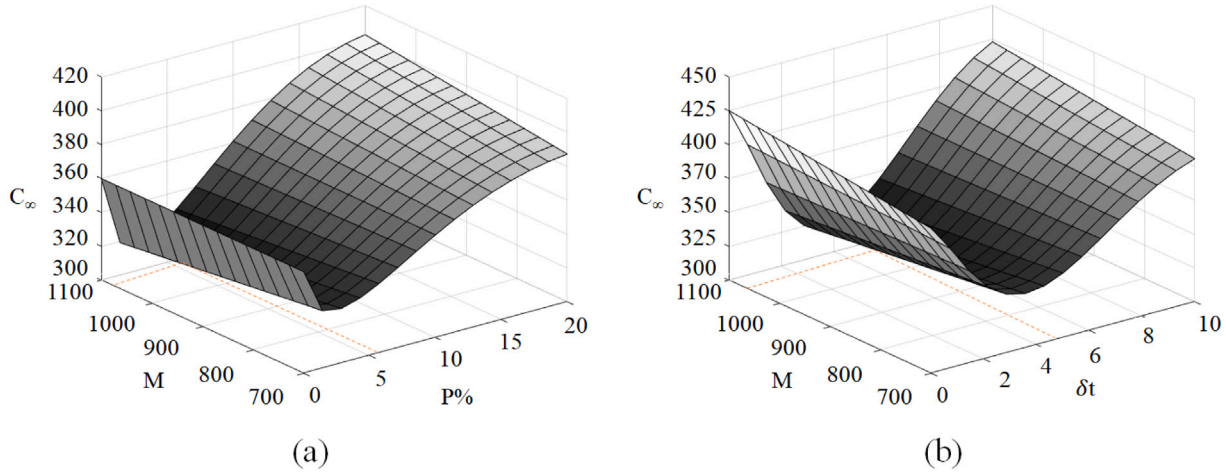


**Fig. 18.** Maintenance cost rate as a function of iterations numbers: (a) the policy ($M$, $P\%$), (b) the policy ($M$, $\delta$).

## References


[1] Yan T, Lei Y, Li N, Wang B, Wang W. Degradation modeling and remaining useful life prediction for dependent competing failure processes. Reliab Eng Syst Saf 2021;212:107638.

[2] Wang C, Elsayed EA. Stochastic modeling of corrosion growth. Reliab Eng Syst Saf 2020;204:107120.

[3] Jahani S, Zhou S, Veeramani D. Stochastic prognostics under multiple time-varying environmental factors. Reliab Eng Syst Saf 2021;107877.

[4] Wen P, Zhao S, Chen S, Li Y. A generalized remaining useful life prediction method for complex systems based on composite health indicator. Reliab Eng Syst Saf 2021;205:107241.

[5] Heidary R, Groth KM. A hybrid population-based degradation model for pipeline pitting corrosion. Reliab Eng Syst Saf 2021;214:107740.

[6] Veloso GA, Loschi RH. Dynamic linear degradation model: Dealing with heterogeneity in degradation paths. Reliab Eng Syst Saf 2021;210:107446.

[7] Xu H, Fard N, Fang Y. Time series chain graph for modeling reliability covariates in degradation process. Reliab Eng Syst Saf 2020;204:107207.

[8] Bogdanoff JL, Kozin F. Probabilistic models of cumulative damage(book). New York: Wiley-Interscience; 1985, p. 350, (1985).

[9] van Noortwijk JM. A survey of the application of gamma processes in maintenance. Reliab Eng Syst Saf 2009;94(1):2–21.

[10] Frangopol DM, Kallen M-J, v. Noortwijk JM. Probabilistic models for life-cycle performance of deteriorating structures: review and future directions. Prog Struct Eng Mater 2004;6(4):197–212.

[11] Abdel-Hameed M. Degradation processes: An overview. In: Advances in degradation modeling. Springer; 2010, p. 17–25.

[12] Ye Z-S, Chen N. The inverse gaussian process as a degradation model. Technometrics 2014;56(3):302–11.

[13] Sun B, Fan X, van Driel W, Cui C, Zhang G. A stochastic process based reliability prediction method for led driver. Reliab Eng Syst Saf 2018;178:140–6.

[14] Park C, Padgett W. Accelerated degradation models for failure based on geometric brownian motion and gamma processes. Lifetime Data Anal 2005;11(4):511–27.

[15] Ling MH, Ng H, Tsui KL. Bayesian and likelihood inferences on remaining useful life in two-phase degradation models under gamma process. Reliab Eng Syst Saf 2019;184:77–85.

[16] Wang X, Xu D. An inverse gaussian process model for degradation data. Technometrics 2010;52(2):188–97.

[17] Dekker R, Plasmeijer RP. Evaluation of a new maintenance concept for the preservation of highways. IMA J Math Appl Bus Ind 1998;9:109–56.

[18] Chhikara R, Folks J. The inverse gaussian distribution as a lifetime model. Technometrics 1977;19(4):461–8.

[19] Liu D, Wang S, Tomovic MM. Degradation modeling method for rotary lip seal based on failure mechanism analysis and stochastic process. Eksploat Niezawodn 2020;22(3).

[20] Li S, Chen Z, Pan E. Step-stress accelerated degradation test plan for generalized inverse gaussian process. J Shanghai Jiaotong Univ 2017;51(2):186–92.

[21] Esmail MA. Experimental performance evaluation of weak turbulence channel models for fso links. Opt Commun 2021;486:126776.

[22] Xu W, Wang W. Rul estimation using an adaptive inverse gaussian model. Chem Eng Trans 2013;33:331–6.

[23] Guo J, Wang C, Cabrera J, Elsayed EA. Improved inverse gaussian process and bootstrap: Degradation and reliability metrics. Reliab Eng Syst Saf 2018;178:269–77.

[24] Sun B, Li Y, Wang Z, Ren Y, Feng Q, Yang D. An improved inverse gaussian process with random effects and measurement errors for rul prediction of hydraulic piston pump. Measurement 2021;173:108604.

[25] Peng C-Y. Inverse gaussian processes with random effects and explanatory variables for degradation data. Technometrics 2015;57(1):100–11.

[26] Seneta E. Fitting the variance-gamma model to financial data. J Appl Probab 2004;177–87.

[27] Fiorani F. Option pricing under the variance gamma process. 2004, Available at SSRN 1411741.

[28] Daal EA, Madan DB. An empirical examination of the variance-gamma model for foreign currency options. J Bus 2005;78(6):2121–52.

[29] Seneta E. The early years of the variance-gamma process. In: Advances in mathematical finance. Springer; 2007, p. 3–19.

[30] Yoo E. Variance gamma pricing of American futures options (Ph.D. thesis), Florida State University; 2008.
[31] Finlay R, Seneta E. Stationary-increment variance-gamma and t models: Simulation and parameter estimation. Internat Statist Rev 2008;76(2):167–86.
[32] Anar H. Credit risk modeling and credit default swap pricing under variance gamma process (Ph.D. thesis), MIDDLE EAST TECHNICAL UNIVERSITY; 2008.
[33] Wallmeier M, Diethelm M. Multivariate downside risk: Normal versus variance gamma. J Futures Mark 2012;32(5):431–58.
[34] Rathgeber AW, Stadler J, Stöckl S. Modeling share returns-an empirical study on the variance gamma model. J Econ Finance 2016;40(4):653–82.
[35] Nitithumbundit T, Chan JS. Ecm algorithm for auto-regressive multivariate skewed variance gamma model with unbounded density. Methodol Comput Appl Probab 2019;1–23.
[36] Madan DB, Seneta E. The variance gamma (vg) model for share market returns. J Bus 1990;511–24.
[37] Madan DB, Milne F. Option pricing with vg martingale components 1. Math Finance 1991;1(4):39–55.
[38] Avramidis AN, Ecuyer PL, Tremblay P-A, et al. Efficient simulation of gamma and variance-gamma processes. In: Winter simulation conference, Vol. 1. 2003, p. 319–26.
[39] Ribeiro C, Webber N. Valuing path-dependent options in the variance-gamma model by monte carlo with a gamma bridge. J Comput Finance 2004;7(2):81–100.
[40] Fu MC. Variance-gamma and monte carlo. In: Advances in mathematical finance. Springer; 2007, p. 21–34.
[41] Madan DB, Carr PP, Chang EC. The variance gamma process and option pricing. Rev Finance 1998;2(1):79–105.
[42] Gradshteyn IS, Ryzhik IM. Table of integrals, series, and products. Academic Press; 2014.
[43] Finlay R, Seneta E. Option pricing with vg–like models. Int J Theor Appl Finance 2008;11(08):943–55.
[44] Le Courtois O, Walter C. The computation of risk budgets under the lévy process assumption. Finance 2014;35(2):87–108.
[45] Cervellera GP, Tucci MP. A note on the estimation of a gamma-variance process: Learning from a failure. Comput Econ 2017;49(3):363–85.
[46] Bee M, Dickson MM, Santi F. Likelihood-based risk estimation for variance-gamma models. Stat Methods Appl 2018;27(1):69–89.
[47] Nitithumbundit T, Chan JS. An ecm algorithm for skewed multivariate variance gamma distribution in normal mean–variance representation. 2015, arXiv preprint arXiv:1504.01239.
[48] Luethi D, Breymann W, Luethi MD. Package 'ghyp'. 2013.
[49] Scott D, Dong CY, Scott MD, RUnit S. Package 'VarianceGamma'. 2018.
[50] Bismut E, Straub D. Optimal adaptive inspection and maintenance planning for deteriorating structural systems. 2021, arXiv preprint arXiv:2102.06016.
[51] Hurd TR. Credit risk modeling using time-changed brownian motion. Int J Theor Appl Finance 2009;12(08):1213–30.
[52] Hurd T, Kuznetsov A. On the first passage time for brownian motion subordinated by a lévy process. J Appl Probab 2009;46(1):181–98.
[53] Li H. First-passage time models with a stochastic time change in credit risk (Ph.D. thesis), Wilfrid Laurier University; 2009.
[54] Fouladirad M, Paroissin C, Grall A. Sensitivity of optimal replacement policies to lifetime parameter estimates. European J Oper Res 2018;266(3):963–75.
[55] Grimstad A-A, Mannseth T. Nonlinearity, scale, and sensitivity for parameter estimation problems. SIAM J Sci Comput 2000;21(6):2096–113.
[56] Mechanical seals in centrifugal pumps. 2020, https://www.advantageengineering.com/fyi/227/advantageFYI227.php.
[57] Centrifugal pump components. 2020, https://boilersinfo.com/centrifugal-pump-components/, accessed: 2020-11-02.
[58] Makarachi P, Mohammad P. Centrifugal pump mechanical seal and bearing reliability optimization. In: Probabilistic safety assessment and management PSAM, Vol. 12. 2014.
[59] Revuz D, Yor M. Continuous martingales and Brownian motion, Vol. 293. Springer Science & Business Media; 2013.